Bioorganic & Medicinal Chemistry 19 (2011) 1285–1297

Contents lists available at ScienceDirect

Bioorganic & Medicinal Chemistry

journal homepage: www.elsevier.com/locate/bmc

Synthesis, physical–chemical characterisation and biological evaluation of novel 2-amido-3-hydroxypyridin-4(1*H*)-ones: Iron chelators with the potential for treating Alzheimer's disease

Alessandra Gaeta [a], Francisco Molina-Holgado [c], Xiao L. Kong [a], Sarah Salvage [a], Sarah Fakih [a], Paul T. Francis [b], Robert J. Williams [d], Robert C. Hider [a,*]

[a] Division of Pharmaceutical Science, King's College, Franklin-Wilkins Building, Waterloo Campus, Stamford Street, London SE1 9NH, UK
[b] Wolfson Centre for Age Related Diseases, King's College, Hodgkin Building, Guy's Campus, London SE1 1UL, UK
[c] Health Sciences Research Centre, Roehampton University, Whitelands College, Holybourne Avenue, London SW15 4SD, UK
[d] Department of Biology and Biochemistry, University of Bath, Claverton Down, Bath BA2 7AY, UK

ARTICLE INFO

Article history:
Received 8 July 2010
Revised 26 November 2010
Accepted 3 December 2010
Available online 13 December 2010

Keywords:
Hydroxypyridin-4-ones
Neurodegeneration
Oxidative stress
β-Amyloid

ABSTRACT

A novel class of 2-amido-3-hydroxypyridin-4-one iron chelators is described. These compounds have been designed to behave as suitable molecular probes which will improve our knowledge of the role of iron in neurodegenerative conditions. Neurodegenerative disorders, such as Alzheimer's disease (AD) and Parkinson disease (PD), can be considered as diverse pathological conditions sharing critical metabolic processes such as protein aggregation and oxidative stress. Interestingly, both these metabolic alterations seem to be associated with the involvement of metal ions, including iron. Iron chelation is therefore a potential therapeutic approach. The physico-chemical (pK_a, pFe^{3+} and log *P*) and biological properties (inhibition of iron-containing enzymes) of these chelators have been investigated in order to obtain a suitable profile for the treatment of neurodegenerative conditions. Studies with neuronal cell cultures confirm that the new iron chelators are neuroprotective against β-amyloid-induced toxicity.

1. Introduction

Oxidative stress, protein aggregation and redox active metal ions can all be considered promising pharmacological targets for the treatment of neurodegeneration.[1] The critical role of iron and copper, in both oxidative stress and protein aggregation processes, renders chelation therapy a sensible therapeutic strategy. A chelating agent suitable for neurodegenerative disorders could have two possible actions: (a) scavenging the free redox active metal present in excess in the brain to form a non toxic metal complex, which is then excreted; and (b) capping the metal at its protein binding site (β-amyloid, α-synuclein), preventing any redox activity.[2] Capping the metal at the protein binding site would be expected to involve additional interactions between the chelating agent and the target protein.

A chelating agent suitable for the treatment of neurodegenerative disorders must fulfil critical requirements, among which blood–brain barrier (BBB) permeability is of uttermost importance. Lipophilicity, expressed as the log *P* value, should represent a compromise between a high BBB penetration and a low liver extraction. Furthermore, with the necessity of ready permeation of the BBB, the size of the chelator should probably be limited to less than 300 Daltons, thereby excluding most hexadentate ligands.[3] The inhibition of iron-containing enzymes, such as tyrosine hydroxylase and lipoxygenase must be kept to a minimum.

There are two general classes of molecule that fit these requirements, 8-hydroxyquinolines and 3-hydroxypyridinones, both classes having been reported to possess potential for the treatment of neurodegenerative disease. Thus, clioquinol (Fig. 1) has been demonstrated to possess beneficial effects in both Alzheimer's disease and Parkinson's disease models[4,5] and also in clinical studies.[6,7] Unfortunately halogenated hydroxyquinolines possess neurotoxic side effects,[8] but these can be avoided by the use of non halogenated analogues, for instance VK-28 and M30 (Fig. 1).[9] In a study centred on rats with 6-hydroxydopamine induced striatal dopaminergic lesions, VK-28 was found to be capable of providing neuroprotection at very low doses.[10]

Hydroxypyridin-4-ones have also been demonstrated to have benefit in the treatment of neurodegeneration, for instance with

Abbreviations: AD, Alzheimer's disease; Aβ, β-amyloid; BBB, blood–brain barrier; CNS, central nervous system; DFO, desferrioxamine; FeNTA, iron nitrilotriacetic acid; HPO, 3-hydroxypyridin-4-one; LDH, lactate dehydrogenase; LO, lipoxygenase; MTT, 3-(4,5-dimethylthiazol-2-yl)-2,5-diphenyltetrazolium-bromide mitochondrial; PD, Parkinson's disease; TH, tyrosine hydroxylase.

* Corresponding author. Tel.: +44 (0) 20 7848 4882; fax: +44 (0) 20 7848 4800.
E-mail address: robert.hider@kcl.ac.uk (R.C. Hider).

0968-0896/$ - see front matter © 2010 Elsevier Ltd. All rights reserved.
doi:10.1016/j.bmc.2010.12.007

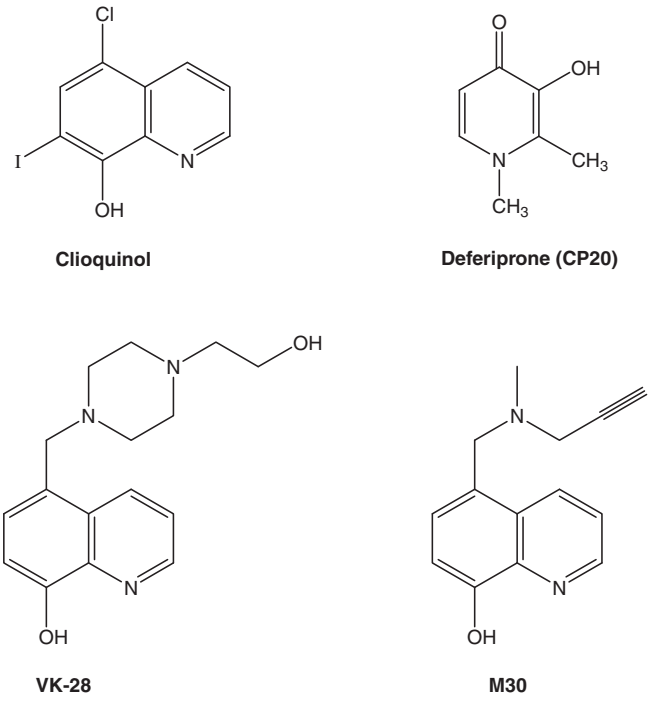

Figure 1. Iron chelators reported to provide protection against neurotoxicity.

Friedrich's ataxia.[11,12] Hydroxypyridin-4-ones are suitable for this purpose, by virtue of their relatively high selectivity for iron(III) and their generally favorable physico-chemical properties. Deferiprone (Fig. 1), a 3-hydroxypyridin-4-one, is a bidentate chelator, which is monoprotic at pH 7.4 and thus forms a neutral tris-iron(III) complex. It has been used clinically for over fifteen years in the treatment of transfusion-induced iron overload.[13] It forms a stable 3:1 ligand iron complex, which is water soluble and readily excreted by the kidneys.[14] Furthermore, deferiprone readily crosses the BBB[15] and has been demonstrated to be neuroprotective against β-amyloid induced neurotoxicity in cortical neuron cultures.[16,17]

In the present work, we have synthesized a small library of highly selective iron(III) hydroxypyridinone-based ligands with suitable physico-chemical, toxicological properties and neuroprotective activity.

The critical involvement of iron in oxidative stress and protein aggregation renders chelation therapy a sensible strategy for the treatment of neurodegenerative disorders in general and of AD in particular.[18] The new library of HPOs described in this work has been specifically designed to possess potential for the treatment of neurodegenerative diseases.

2. Results and discussion

2.1. Chemistry

The synthesis of acid **9**, a key building block**,** is summarised in Scheme 1 and follows the procedure described by Piyamogkol et al.[19] Compounds **10a–k** were prepared from the Z-protected amino acids glycine, alanine and phenylalanine by reaction with the suitable amine following optimised reaction conditions, using either EDC or DCCI as coupling reagents. Deprotection of compounds **10a–k** by hydrogenation, using palladium as the catalyst, afforded the free amines **11a–k**, which were subsequentially reacted with compound **9** using DCCI to afford intermediates **12a–k** (Scheme 2). Compound **14** (Scheme 3) was obtained by treating **12a** with a large excess of methyl iodide under reflux. Finally, compounds **12a–k** and **14** were deprotected using boron trichloride to afford the desired chelating agents **13a–l** and **15**. (Schemes 2 and 3).

2.2. Physico-chemical properties of iron probes: iron affinity (pM) and lipophilicity (log *D* and HPLC estimated log *P*)

Under biological conditions the pM value is a more useful parameter than the conventional stability constant for the assessment of the ligand affinity for metals.[20,3] The pM values of the newly synthesised HPOs fall in a range, pFe^{3+} = 18.9–21.5, which is consis-

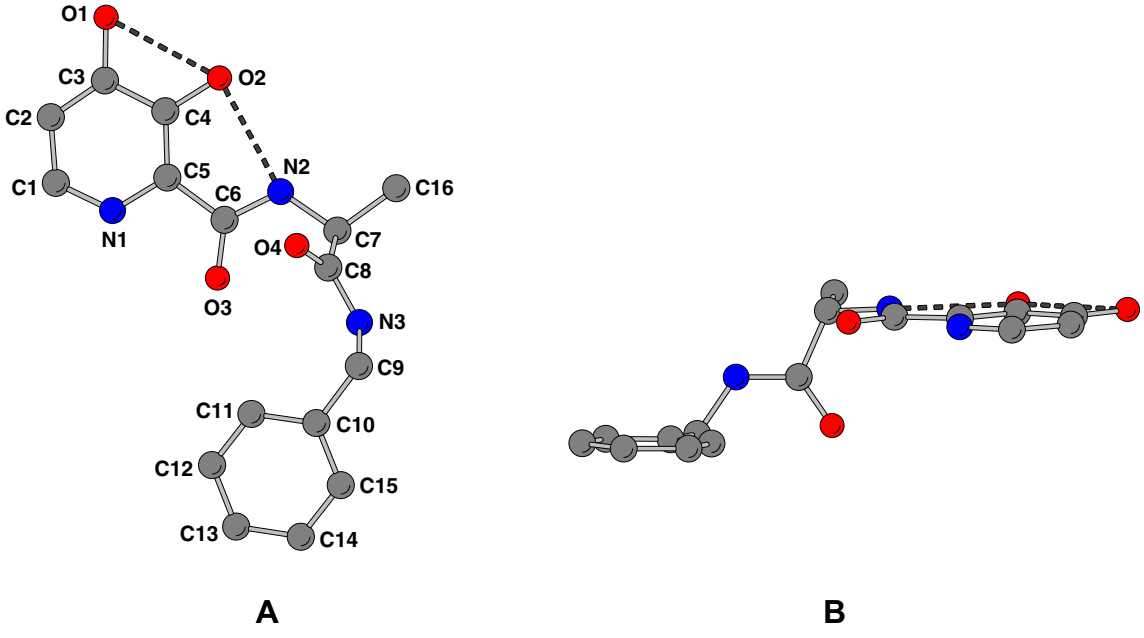

Figure 2. (A and B) Crystal structure of compound **13f**. (A) the free ligand is shown. H-bonding between N2 and O2 is highlighted; (B) compound **13f** spatial arrangement. The chelation moiety is planar and parallel to the plane of the benzyl group.

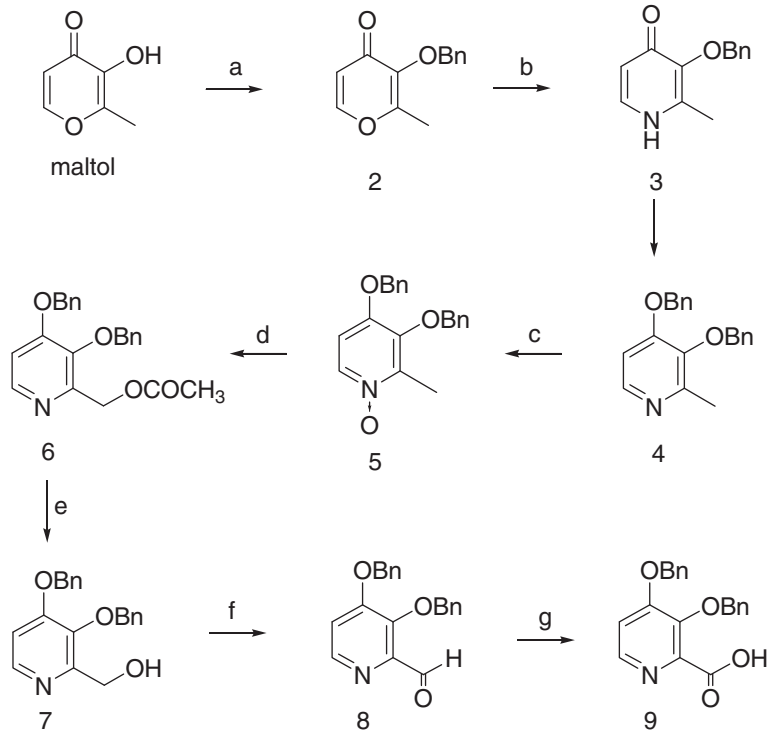

Scheme 1. Synthesis of Intermediate **9**. Reagents and conditions: (a) Benzyl bromide, NaOH, methanol, reflux, 6 h; (b) ammonia, ethanol, reflux, overnight; (c) triphenylphosphine, DEAD, THF, benzyl alcohol, reflux, overnight; (d) MCPBA, DCM, rt, 4 h; e) acetic anhydride, reflux, 2 h; (f) 2 N NaOH, reflux, 1 h; (g) DMSO, py-SO_3, TEA, Chloroform, rt, overnight; (h) $NaClO_2$, NH_2SO_3H, acetone/water 1:1, rt, 3 h.

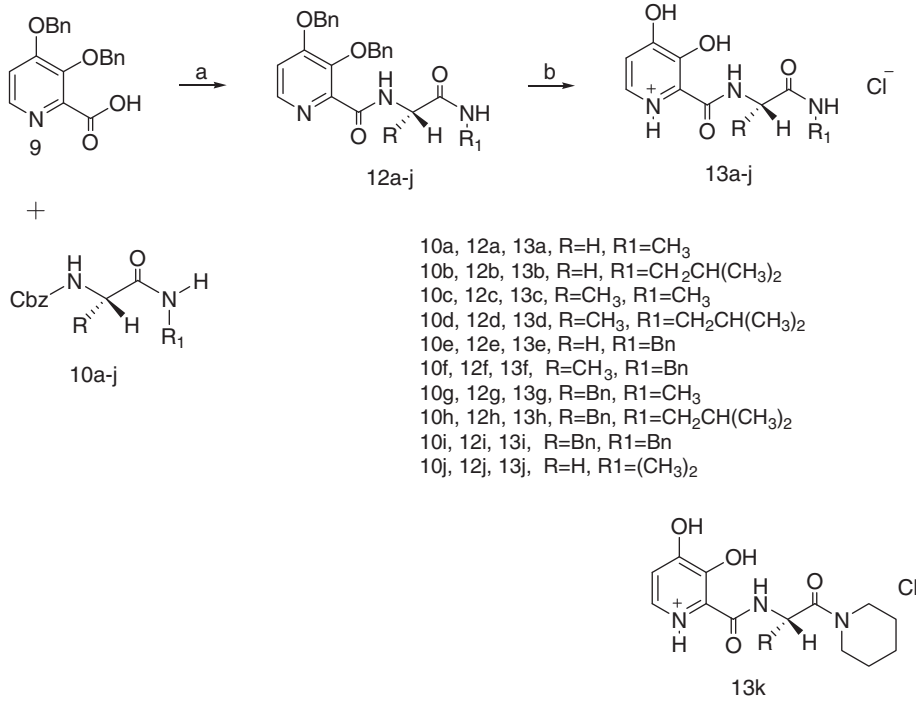

Scheme 2. Synthesis of iron chelators **13a–k**. Reagents: (a) DCC, HOBt, DCM; (b) BCl_3, DCM.

tent with high affinity iron(III) ligands (Table 1). Typically, for clinically useful iron scavengers, a pFe^{3+} value $\geqslant 20$ is considered to be essential.[3] When compared to deferiprone (pFe^{3+} = 19.4), the new compounds show a good affinity for iron, with compounds **13g** and **13i** having pFe^{3+} values of 21.4 and 21.5, respectively. The potentiometric determination of one of these compounds, **13c**, is presented in Figure 3. Interestingly, compounds **13c**, 13d and **13f** (alanine derivatives) have consistently lower pFe^{3+} values (19.1, 19.2 and 18.9, respectively), compared to the corresponding glycine analogues **13a**, 13b and **13e**, (20.8, 20.6 and 19.1, respectively) and phenylalanine analogues **13g**, 13h and **13i** (21.4, 20.4 and 21.5, respectively), suggesting that the methyl group might force the

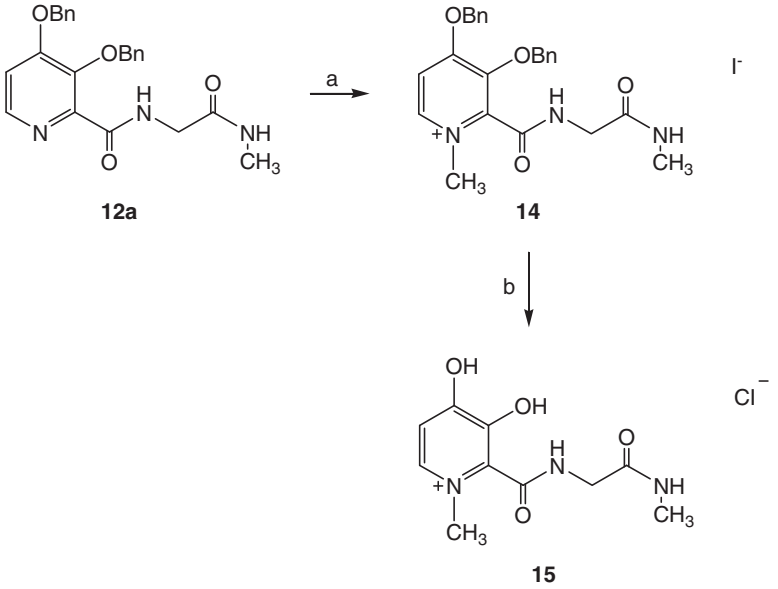

Scheme 3. Synthesis of iron chelator **15**. Reagents: (a) methyl iodide, reflux; (b) BCl_3, DCM

Table 1
Physico-chemical properties of novel iron chelators

Compound	pK_a	pFe^{3+}	log *D*
13a	6.3	20.8	−1.42
13b	6.2	20.6	−0.33
13c	6.0	19.1	−1.1
13d	6.0	19.2	−0.08
13e	6.2	19.1	0.01
13f	6.0	18.9	0.03
13g	6.1	21.4	−0.11
13h	6.0	20.4	0.39
13i	6.0	21.5	0.90
15	–	–	−1.08[a]

[a] Log *P* value was estimated by HPLC.

ligand to adopt a different conformation. The crystal structure of compound **13f** shows the formation of an intramolecular hydrogen bond between the amide NH and the 'catechol' hydroxyl group (Fig. 2, Table 2). It is likely that the same hydrogen bond would form in all the derivatives, thereby stabilising the ionised species at physiological pH values and influencing the affinity for iron(III).

The lipophilicity of the novel compounds was assessed by the *shake-flask* method (log *D*) and by HPLC (estimated log *P*). All the compounds in the series have log *D* values (0.90–1.52) (Table 1) falling in a range of lipophilicity, which is predicted to permit good blood–brain barrier permeability. A good correlation was found between the determined log *D* values using the *shake-flask* method and the log *P* values estimated using regression analysis of HPLC retention times. Using this approach, the log *P* value for compound **15** was estimated to be –1.08 (retention time 3.87 min) as shown in Figure 4. The log *D* for **15** could not be determined using the *shake-flask* method due to the relative insolubility of the compound in *n*-octanol. The estimated log *P* value appears to be consistent with the introduction of an extra methyl group, when compared to compound **13a**, the non-methylated analogue having a log *D* value of −1.52.

2.3. Lipoxygenase and tyrosine hydroxylase inhibition

The compounds have been tested to evaluate inhibitory activity on the iron containing enzymes lipoxygenase and tyrosine hydroxy-

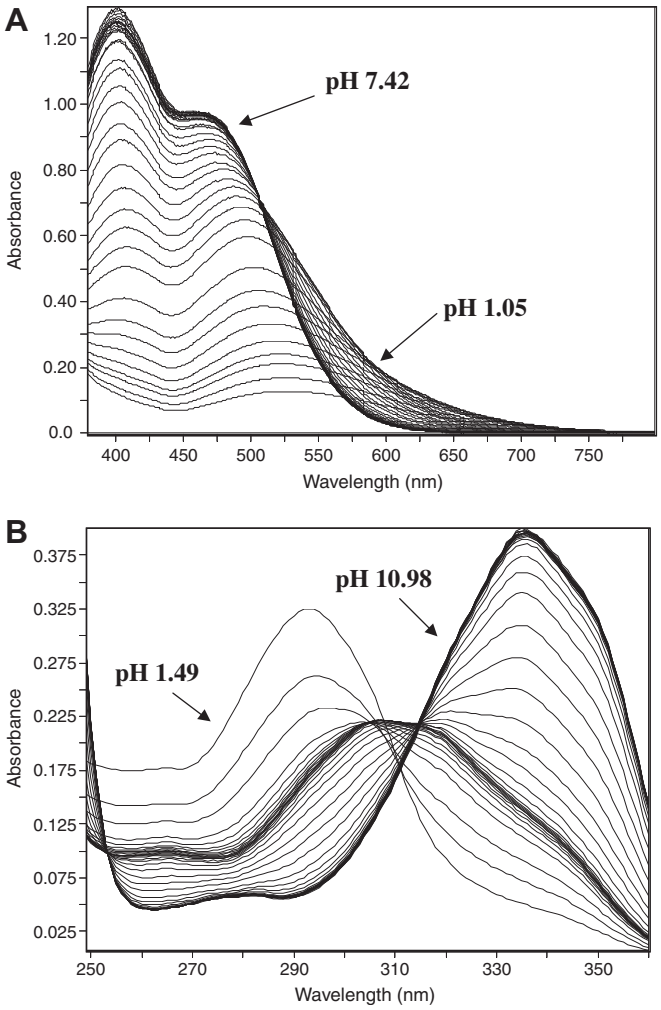

Figure 3. (A) pH dependence of the spectrum of ligand **13c** in the presence of iron(III) over the pH range 1.05 and 7.42 in 0.1 M KCl at 25 °C [Fe] = 37.2 μM [**13c**] =186 μM. (B) pH dependence of the spectrum of ligand **13c** over the pH range 1.49 and 10.98. [**13c**] = 4.68×10^{-4} M.

Table 2
Crystal data and structure refinement

Empirical formula	$C_{16}H_{18}ClN_3O_4$
Formula weight (g/mol)	351.79
Crystal system	orthorhombic
Space group	$P2_12_12_1$ (No. 19)
Unit cell dimensions	
a (Å)	6.7608(1)
b (Å)	12.8465(1)
c (Å)	19.4017(2)
α (°)	90
β (°)	90
γ (°)	90
Volume (Å^3)	1685.09(3)
Formula units/cell	8
D_c (g/cm^3)	1.387
Diffractometer (wavelength, Å)	BRUKER AXS SMART 6000 (Cu-Kα, λ = 1.54178)
Monochromator	Göbel mirror
Temperature (K)	293(2)
Absorption coefficient (mm^{-1})	2.237
Data collection range	$8.26° < 2\theta < 142.86°$
Indices	$-8 \leqslant h \leqslant 7$ $-15 \leqslant k \leqslant 15$ $-21 \leqslant l \leqslant 23$
Reflections collected	9787
Independent reflections	3118 [$R_{(int)}$ = 0.1417]
Program for structure solution	SHELXS-97
Program for structure refinement	SHELXL-97
Goodness-of-fit on F^2	1.054
Final *R* values ($I > 2\sigma$ (I))	R_1 = 0.0416, wR_2 = 0.1064
Final *R* value (all data)	R_1 = 0.0421, wR_2 = 0.1070
$(\Delta/\rho)_{max}$; $(\Delta/\rho)_{min}$ (e Å^{-3})	0.301; −0.427

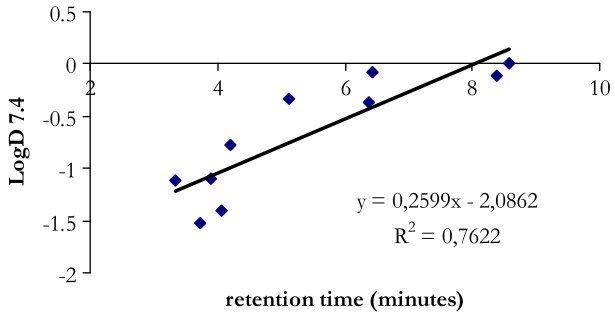

Figure 4. Regression analysis for estimation of log *P* for compound **15**. The retention time of the compound was determined as 3.87 min. This was plotted against log *D* values determined for other compounds in the series. The estimated log *P* value was calculated using the above equation.

lase, with the second enzyme being particularly relevant in the context of neurodegenerative disease. An important contribution to the toxicity associated with iron chelators is associated with their ability to inhibit metallo-enzymes.[21–23] In general, iron chelators do not directly inhibit heam iron-containing enzymes due to the inaccessibility of porphyrin-bound iron, however many non-heam iron-containing enzymes are susceptible to such inhibition.[24]

Generally, hydrophobic chelators inhibit the lipoxygenase family of enzymes,[22,23] therefore the introduction of hydrophilic groups into the chelator structure has a tendency to minimise such potential, particularly if these substituents also create a steric interference in the chelation at the enzyme active site.[21] This concept has been confirmed in this study, where none on the newly described compounds were found to possess appreciable lipoxygenase inhibitory activity. Thus, compound **13f** does not show comparable inhibition activity on LO to that of CP27, which was used in this study as a positive control.

Table 3
Inhibition of lipoxygenase enzyme

Compound	EC_{50} (μM)	%Inhibition (100 μM)	%Inhibition (10 μM)
CP94	11	87.4[a], 92	43
CP20	64	75.3[a], 58	—
13a	56	68	19.3
13b	44	70	9.3
13c	66	61	2.7
13d	37	71	15.3
13e	54	62	8.3
13f	80	54	3.3
13g	25	71	27.6
13h	13	81	46.5
13i	52	60	30.2

The EC_{50} is an indicative value, not necessarily reflecting the actual IC_{50}, because the maximal inhibition is not achieved at 100 μM for all the compounds.
[a] Published values.

In an analogous fashion, lipophilicity is a dominant factor in influencing the ability of HPOs to inhibit mammalian tyrosine hydroxylase, typically hydrophilic chelators are weak inhibitors.[25] Within the present HPO series, **13f** and **13c** were found to be weak inhibitors at 10 μM, whereas **13g**, **13h** and **13j**, the more lipophilic derivatives, had a considerable inhibitory effect on the enzyme at this concentration (Table 3 and Fig. 5).

2.4. In vitro neuroprotective activity of new iron chelators

The chelators have been evaluated for neuroprotective activity in cultured primary mouse cortical neurons, against two types of insult: the presence of either iron (FeNTA) or amyloid-β 1–40 (Aβ1–40). The neuroprotective effect of iron chelation displayed by the novel compounds in the FeNTA model was evaluated by assessing LDH release into the media and MTT turnover within cells and by the preservation of synaptic integrity after exposure of cortical neurones to FeNTA (10 μM) for 6 h prior to addition of the drug. In the absence of drug, the exposure of neurons to FeNTA led to a large increase in LDH levels in the media reflecting damage to the neuronal cell membrane. This increase was significantly reduced by compounds **13b**, **13f** and **13g** at concentrations of 30 μM and above and also by **13i** at 100 μM (Table 4). In the absence of drug, the exposure of neurons to FeNTA led to a large reduction in MTT turnover reflecting impaired mitochondrial respiration and reduced viable cell number. This reduction was significantly reversed by **13a**, **13b**, **13f** and **13g** at concentrations of 30 μM and above (not shown). The greatest overall level of protection, as assessed by either LDH release or MTT turnover, was observed with compound **13f** (Fig. 6) which was, therefore taken forward for further analysis. Morphological assessment of neurons, following exposure to FeNTA in the absence of drug, showed damage to cell bodies and a loss of neuritis implying damage to synapses (Fig. 7A). Damage to synapses was confirmed by a substantial reduction in the levels of the nerve terminal marker synaptophysin (Fig. 7B and C). Cell damage and reduction in synaptophysin levels were reversed by **13f** at concentrations of 30 μM and 100 μM (Fig. 7A–C).

The neuroprotective actions of **13f** were also evaluated against synthetic human Aβ1–40 induced toxicity. In this model, neurons were exposed to **13f** (10 μM, 30 μM and 100 μM) or Aβ1–40 (3 μM and 20 μM) alone or in combination for 24 h and neuronal cell viability assessed by Hoe33342 and propidium iodide double labelling (Fig. 8). Exposure to Aβ1–40 in the absence of **13f** caused a dramatic increase in propidium iodide staining and a reduction in Hoe33342 indicating high levels of cell death. **13f** had no effect on cell viability alone but reversed Aβ-induced toxicity at concentrations of 10 μM and above.

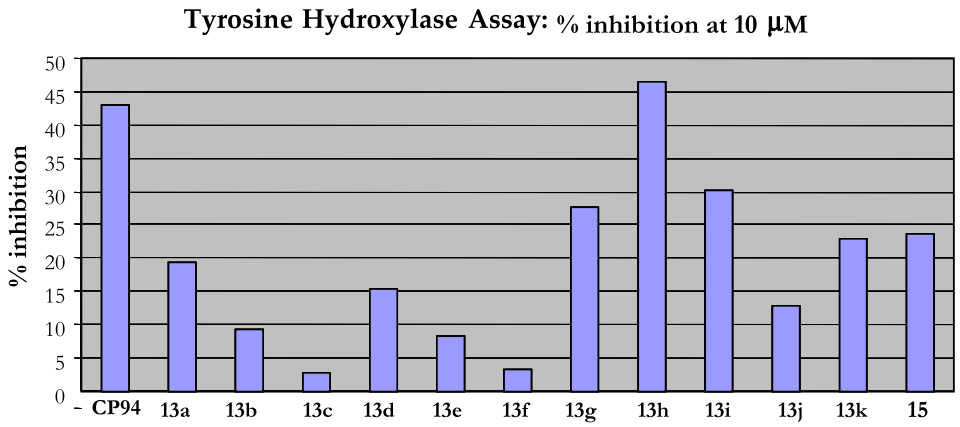

Figure 5. Compounds **13a–l** and **15** inhibitory activities against tyrosine hydroxylase enzyme at 10 μM are compared to potent inhibitor **CP94**.

Table 4
Protection of cultured cortical neurons against FeNTA-induced cell death

Compound	Control	FeNTA (10 μM)	FeNTA (10 μM) + [Chelator] (μM)			%Protection at 100 μM
			10	30	100	
13a	34.18 ± 2.22	86.36 ± 13.05	58.41 ± 18.85	46.52 ± 13.27	46.10 ± 4.15	77
13b	35.87 ± 2.17	87.05 ± 6.94	70.32 ± 3.95	61.16 ± 4.43*	56.44 ± 7.46*	60
13c	34.85 ± 1.45	85.45 ± 8.16	66.52 ± 10.91	61.96 ± 9.95	56.22 ± 5.49	58
13d	34.42 ± 1.27	79.48 ± 13.44	64.55 ± 10.07	54.73 ± 6.37	54.08 ± 7.78	56
13e	34.42 ± 1.27	79.48 ± 13.44	65.67 ± 11.89	56.62 ± 9.46	47.77 ± 7.22	70
13f	37.01 ± 1.26	77.79 ± 4.75	69.79 ± 2.41	52.49 ± 4.05**	42.41 ± 1.16**	87
13g	37.01 ± 1.26	77.79 ± 4.75	70.03 ± 1.50	48.9 ± 2.70**	45.80 ± 1.00**	78
13h	35.92 ± 0.32	79.97 ± 5.08	72.83 ± 1.69	53.8 ± 8.74	53.30 ± 7.57	61
13i	37.31 ± 1.10	82.36 ± 2.75	76.87 ± 3.94	64.85 ± 5.61	54.59 ± 3.14**	62
15	33.81 ± 3.55	101.40 ± 0.54	94.50 ± 0.88	94.52 ± 0.84	93.36 ± 0.98	12

Data represents the mean release of lactate dehydrogenase into the growth medium as a % of total cellular LDH (=100%) ± SEM, $n = 4$.
*p <0.05; **p <0.01 One Way ANOVA.

This study demonstrates that in an in vitro model of neuronal death, a range of novel 2-amido-3-hydroxypyridin-4-one iron chelators provide neuroprotection. Cortical neurons cultures have proved to be useful models for studying the underlying mechanisms to cell death. In this study several mechanisms of neuronal damage have been investigated, leading to important observations. First, FeNTA induced significant death of primary cortical neurons in a concentration-dependent manner, which was reversed by iron chelators in a concentration-dependent fashion. This concentration-dependent effect probably is a consequence of the neuronal uptake of ferric iron, although an extracellular mode of action may also be a factor. Furthermore, it is interesting to note that a number of the chelators were capable of providing neuroprotection for periods up to 6 h after the neuronal cultures had been exposed to FeNTA. This finding is potentially of clinical interest, as it suggests that iron chelation may provide protection post-insult, not only in chronic neurodegeneration but also in acute conditions involving iron, such as cerebral ischemia/stroke.[26]

One of the mechanisms of cytotoxicity induced by iron is the disruption of the synaptic organization. In this study, we provide evidence that the iron chelators **13c** (not shown) and **13f** preserve synapses against iron-induced damage by preservation of the levels of synaptophysin (Fig. 7B), a key synaptic structural protein.[27] Recent evidence indicates that over-expression of synaptophysin attenuates neurotoxicity.[28]

Despite the well established protective effects of iron chelation in different pathologies,[29] these findings, taken together with the previous work with Deferiprone,[16,17] provide the first example where a clear connection is made between neuroprotection and iron chelation.

Furthermore, the in vitro approach on primary neuronal cultures using Aβ1–40 enabled a specific analysis of the cellular processes responsible for both neuronal vulnerability in response to an insult which requires redox active iron.

AD is associated with elevated soluble and aggregated forms of both Aβ1–40 and Aβ1–42 and oxidative stress[30] and there is increasing evidence for a detrimental role of iron in the pathogenic process.[31,32] This study clearly demonstrates that Aβ (3 or 10 μM) induced neuronal cell death was abolished by treatment with low concentrations of iron chelators, suggesting a role for iron in the observed Aβ neurotoxic effects. As a consequence, the use of iron chelators may offer therapeutic advances in the treatment of neurodegenerative disorders related to amyloid toxicity.

3. Conclusions

In summary, new iron bidentate chelators belonging to the family of 2-amido-3-hydroxypyridin-4-one show potential as non-toxic therapeutic agents for the treatment of neurodegenerative disorders.

Although much needs to be understood in terms of the etiopathogenesis of neurodegeneration, it is clear from this study that chelation therapy can be considered as a potential strategy for the treatment and investigation of neurodegeneration.

4. Experimental

4.1. Chemistry

Melting points were determined using an Electrothermal IA 9100 Digital Melting Point Apparatus and are uncorrected. IR spectra were performed on a Perkin–Elmer 1605 FTIR. ^{1}H NMR spectra were recorded on a Bruker (360 MHz) spectrometer. Chemical

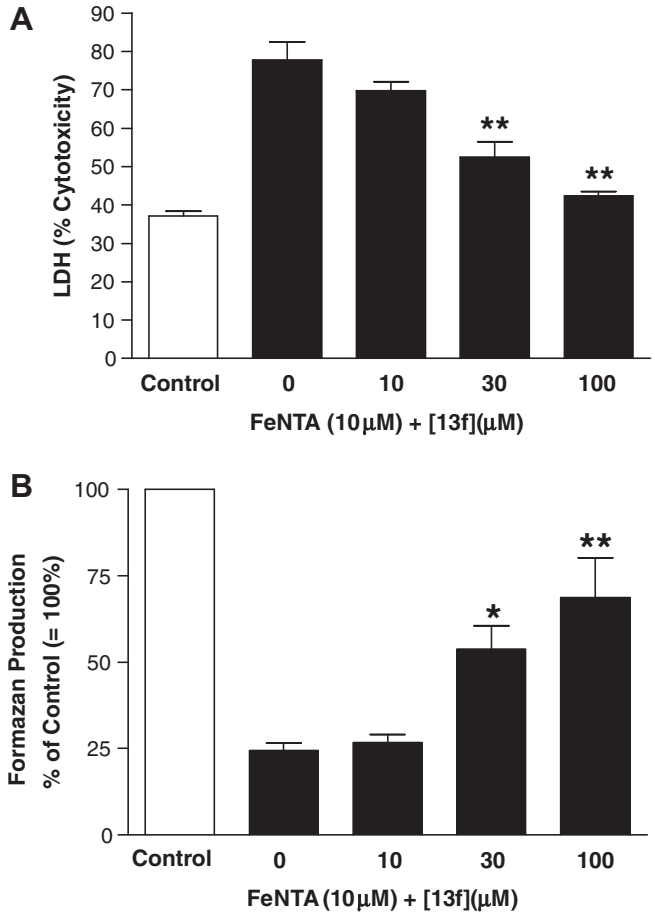

Figure 6. Compound **13f** protects cortical neurons against FeNTA-induced neurotoxicity in a concentration-dependent manner. Neurons were exposed to FeNTA (10 μM) for 6 h before the addition of **13f** for a further 18 h. Neuronal viability was then assessed by LDH release (A) and by MTT turnover (B). Compound **13f** protected neurones against FeNTA toxicity at concentrations of 30 μM and 100 μM. $^{*}p$ <0.05, $^{**}p$ <0.01, n = 4; One Way ANOVA.

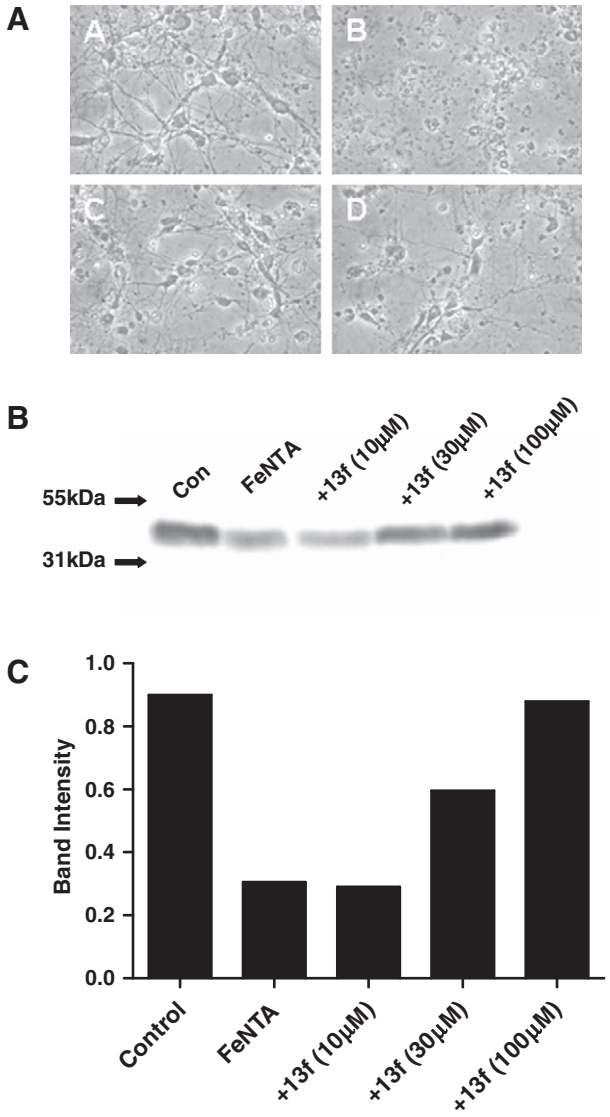

Figure 7. Compound **13f** protects cortical neurons against FeNTA-induced loss of synaptic integrity. Upper panel (A) shows phase contrast images of neurons treated with vehicle (A), FeNTA (10 μM) alone (B), FeNTA with **13f** (30 μM) (C) or FeNTA with **13f** (100 μM). Immunoblot (B) shows levels of synaptophysin in neuronal lysates following treatment with vehicle (Con), or FeNTA (10 μM) with or without increasing concentrations of **13f**. Arrows indicate position of molecular weight markers. Graph (C) shows quantification of the immunoreactive bands shown in B using image J densitometric analysis.

shifts (δ) are reported in ppm downfield from the internal standard tetramethylsilane (TMS). Mass spectra (ESI) analyses were carried out by Mass Spectrometry Facility, School of Health and Science, Franklin-Wilkins Building, King's College, London SE1 9NH. All starting materials were obtained from commercial sources and used without further purification. 3-Hydroxy-2-methyl-4*H*-pyran-4-one (maltol, **1**) was purchased from Cultor Food Science. Column chromatography was performed on silica gel 220–440 mesh (Fluka). All the biologically tested compounds (**13a**–**k** and **15**) were tested for purity by HPLC and were found more than 95% pure. HPLC method & column: 5–95% acetonitrile/water gradient over 30 min on Luna C18, 10 μ, 250 × 4.6 mm at 254 nm wavelength.

4.1.1. 2-Methyl-3-benzyloxypyran-4(1*H*)-one (2)

To a solution of maltol (1) (10 g, 0.079 mol) in methanol (20 mL) was added sodium hydroxide (3.49 g, 0.087 mol, 1.1 equiv) in water (10 mL). The reaction mixture was heated to reflux before benzyl bromide (10.4 mL, 0.087 mol, 1.1 equiv) was slowly introduced dropwise and the mixture was left to reflux for 6 h. After the solvent was removed, the residue was taken into water and dichloromethane. The aqueous fraction was discarded and the organic fraction washed with sodium hydroxide 5% (3×) followed by water (2×). The combined fractions were dried over anhydrous sodium sulfate, filtered, and evaporated under reduced pressure. Re-crystallisation from diethyl ether afforded off-white crystals, mp 54–56 °C. Yield 80%. ^{1}H NMR ($CDCl_3$) δ 2.07 (3H, s, CH_3), 5.15 (2H, s, CH_2Ph), 6.36 (1H, d, J = 5.7 Hz, 5-*H*), 7.31–7.40 (5H, m, CH_2*Ph*), 7.59 (1H, d, J = 5.7 Hz, 6-*H*); m/z (ESI): 202.0.

4.1.2. 2-Methyl-3-benzyloxypyridin-4(1*H*)-one (3)

To a solution of 2 (13.8 g, 0.064 mol) in ethanol (25 mL) was added ammonia solution (50 mL) and refluxed overnight. The solvent was removed under reduced pressure, then taken into water and adjusted to pH 1 with concentrated hydrochloric acid. The aqueous mixture was washed with ethyl acetate (3×) and the pH was adjusted to pH 10 with sodium hydroxide (2 M.). The aqueous phase was extracted with chloroform (3×), dried over anhydrous sodium sulfate, filtered, and evaporated under reduced pressure. Re-crystallisation from methanol/diethyl ether gave brown cubic crystals, mp 162–164 °C. Yield 75%. ^{1}H NMR ($CDCl_3$) δ 2.15 (3H,

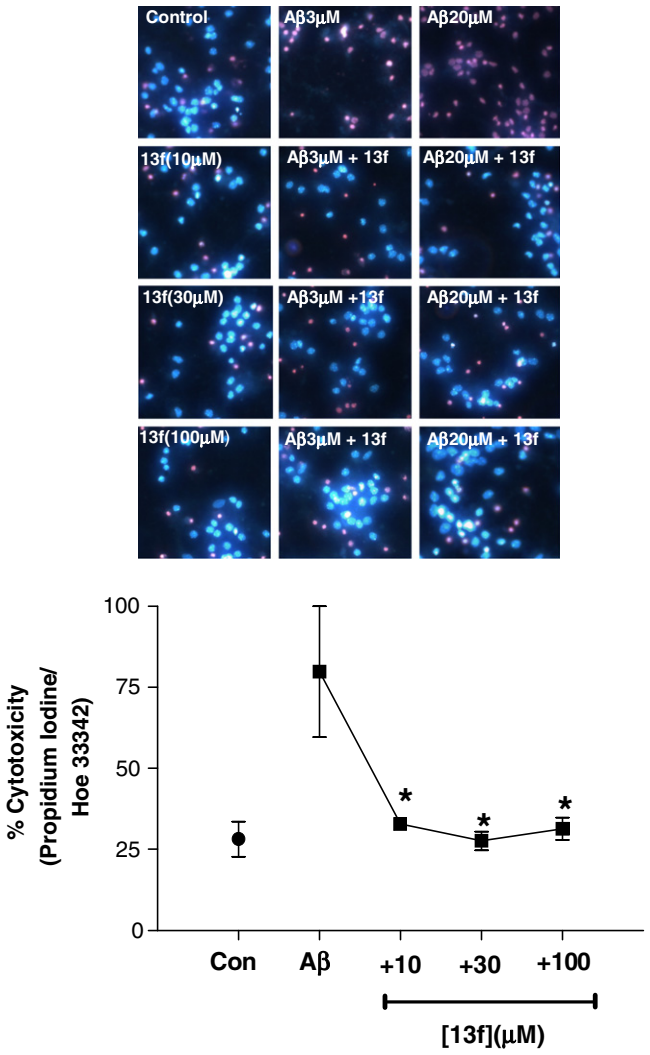

Figure 8. Compound **13f** protects cortical neurons against Aβ1–40 induced toxicity. Neurons were exposed to **13f** (10 μM, 30 μM and 100 μM) or Aβ1–40 (3 μM and 20 μM) alone or in combination for 24 h and neuronal cell viability assessed by Hoe33342 (blue) and propidium iodide (purple) double labelling. Data was captured using an *In Cell* Analyser and % cytotoxicity calculated as number of propidium iodide positive cells relative to the number of Hoe33342 positive cells. Compound **13f** significantly reduced Aβ toxicity. $^{*}p$ <0.05, One Way ANOVA.

s, C*H*$_3$), 5.03 (2H, s, C*H*$_2$Ph), 6.35 (1H, d, *J* = 6.9 Hz, 5-*H*), 7.25–7.31 (5H, m, CH$_2$*Ph*), 7.39 (1H, d, *J* = 6.9 Hz, 6-*H*); *m*/*z* (ESI): 201.1.

4.1.3. 2-Methyl-3,4-dibenzyloxypyridine (4)

Triphenylphosphine (TPP) (2.9 g, 11.16 mmol, 1.2 equiv) was slowly added to a solution of 3 (2 g, 9.30 mmol) in dry tetrahydrofuran (20 mL), and the solution was cooled to 0 °C in ice bath. Benzyl alcohol (1.2 g, 11.16 mmol, 1.2 equiv) was later introduced dropwise followed by diethylazodicarboxylate (DEAD) (1.9 g, 11.16 mmol, 1.2 equiv) in the same manner. After refluxing the reaction mixture overnight, the solvent was removed under reduced pressure and the residue was extracted with water. The mixture was adjusted to pH 1 with concentrated hydrochloric acid before washing with diethyl ether (4×). The pH of the aqueous fraction was increased to 8 with sodium hydroxide (2 M.), followed by extraction with ethyl acetate (4×). The combined organic fractions were dried over anhydrous sodium sulfate, filtered, and concentrated under reduced pressure to give a white solid. Recrystallisation from chloroform/petroleum spirit gave white crystals, mp 85–87 °C. Yield 79%. ν_{max} (KBr) 3264 (ring C–H), 1589, 1498, 1485 and 1449 (ring C=C), 1218 and 1066 (C–O–C) cm^{-1}. ^{1}H NMR (CDCl$_3$) δ 2.43 (3H, s, C*H*$_3$), 5.00 (2H, s, 3-OC*H*$_2$Ph), 5.17 (2H, s, 4-OC*H*$_2$Ph), 6.79 (1H, d, *J* = 5.6 Hz, 5-*H*), 7.30–7.45 (10H, m, 3-OCH$_2$*Ph* and 4-OCH$_2$*Ph*), 8.13 (1H, d, *J* = 5.6 Hz, 6-*H*); *m*/*z* (ESI): 290.8.

4.1.4. 2-Methyl-3,4-dibenzyloxypyridine *N*-oxide (5)

A solution of *m*-chloroperoxybenzoic acid (MCPBA) (0.622 g, 3.63 mmol, 1.1 equiv) in dichloromethane (20 mL) was prepared and cooled to 0 °C. A solution of 4 (1 g, 3.3 mmol) in dichloromethane (5 mL) was added slowly. The reaction mixture was left to stir at room temperature for 3 h prior to addition of dichloromethane (20 mL) to increase the volume. The solution was washed with sodium carbonate (5%, 3×). The organic phase was dried over anhydrous sodium sulfate, filtered, and concentrated under reduced pressure to give yellow oil. Crystallisation in the form of white fluffy powder resulted subsequent to the addition of diethyl ether, mp 127–129 °C. Yield 77%. ν_{max} (KBr) 3245 (ring C–H), 3041 and 2991 (aliphatic C–H), 1533 (ring C=C), 1240 and 1068 (C–O–C) cm^{-1}. ^{1}H NMR (CDCl$_3$) δ 2.40 (3H, s, C*H*$_3$), 5.05 (2H, s, 3-OC*H*$_2$Ph), 5.17 (2H, s, 4-OC*H*$_2$Ph), 6.74 (1H, d, *J* = 7.3 Hz, 5-*H*), 7.32–7.41 (10H, m, 3-OCH$_2$*Ph* and 4-OCH$_2$*Ph*), 8.04 (1H, d, *J* = 7.3 Hz, 6-*H*); *m*/*z* (ESI): 306.9.

4.1.5. 2-Acetoxymethyl-3,4-dibenzyloxypyridine (6)

Acetic anhydride (20 mL) was added into a flask containing 5 (1 g, 3.10 mmol) and the reaction mixture was heated to 130 °C for 1 h. The solvent was removed under reduced pressure and the residue dissolved in water. The pH of the solution was adjusted to 8 with sodium hydroxide (2 M) and was then extracted with dichloromethane (3×). The organic fractions were dried over anhydrous sodium sulfate, filtered, and concentrated in vacuo to yield brown oil. Treatment with decolourising charcoal yielded yellow oil. ^{1}H NMR (CDCl$_3$) δ 2.07 (3H, s, OCOC*H*$_3$), 5.08 (2H, s, 3-OC*H*$_2$Ph), 5.18 (2H, s, 4-OC*H*$_2$Ph), 5.20 (2H, s, C*H*$_2$OCOMe), 6.91 (1H, d, *J* = 5.6 Hz, 5-*H*), 7.30–7.48 (10H, m, 3-OCH$_2$*Ph*, 4-OCH$_2$*Ph*), 8.25 (1H, d, *J* = 5.6 Hz, 6-*H*); *m*/*z* (ESI): 305.1.

4.1.6. 2-Hydroxymethyl-3,4-dibenzyloxypyridine (7)

To a solution of 2-acetoxymethyl-3,4-dibenzyloxypyridine (1.14 g, 3.13 mmol) in ethanol (10 mL), sodium hydroxide (2 M, 7 mL) was added and the reaction mixture refluxed for 2 h. The product was extracted with dichloromethane (4×), dried over anhydrous sodium sulfate, filtered, and concentrated under reduced pressure to give an off-white solid (81% overall yield in two steps). Re-crystallisation from diethyl ether/petroleum spirit gave an off-white fluffy powder, mp 83–85 °C; ν_{max} (KBr) 3165 (br, O–H), 2954 (aliphatic C–H), 1595 (ring C=C), 1301 and 1035 (C–O–C) cm^{-1}. ^{1}H NMR (CDCl$_3$) δ 3.69 (1H, s, CH$_2$O*H*), 4.65 (2H, s, C*H*$_2$OH), 5.06 (2H, s, 3-OC*H*$_2$Ph), 5.21 (2H, s, 4-OC*H*$_2$Ph), 6.89 (1H, d, *J* = 5.5 Hz, 5-*H*), 7.32–7.52 (10H, m, 3-OCH$_2$*Ph*, 4-OCH$_2$*Ph*), 8.19 (1H, d, *J* = 5.5 Hz, 6-*H*); *m*/*z* (ESI): 320.8.

4.1.7. 2-Formyl-3,4-dibenzyloxypyridine (8)

To a solution of 7 (8 g, 0.025 mol) in chloroform (138 mL), was added dimethyl sulfoxide (DMSO) (37 mL) and triethylamine (TEA) (21 mL, 6 equiv). The reaction mixture was then cooled in an ice-bath followed by the slow addition of sulfur trioxide pyridine complex (20 g, 0.125 mol, 5 equiv). The mixture was allowed to thaw at room temperature and left to stir overnight. Water (2×) was used to wash the organic fraction, which was subsequently dried over anhydrous sodium sulfate, filtered, and concentrated in vacuo. The dark green residue obtained was loaded on to a silica gel column (eluant: chloroform/methanol/ethyl acetate; 45:5:50 v/v) to yield an off-white solid. Yield 62%. Recrystallisation from chloroform/petroleum spirit yielded off-white fluffy crystals: mp 103–104 °C; ν_{max} (KBr) 3065 and 3031 (ring C–H), 2858 (aldehyde

C–H), 1709 (aldehyde C=O), 1573 (ring C=C), 1251 and 1043 (C–O–C) cm^{-1}. ^1H NMR ($CDCl_3$) δ 5.19 (2H, s, 3-OCH_2Ph), 5.23 (2H, s, 4-OCH_2Ph), 7.07 (1H, d, J = 5.3 Hz, 5-*H*), 7.31–7.46 (10H, m, 3-OCH$_2$*Ph* and 4-OCH$_2$*Ph*), 8.40 (1H, d, J = 5.3 Hz, 6-*H*), 10.24 (1H, s, C*H*O); *m*/*z* (ESI): 318.8.

4.1.8. 2-Carboxy-3,4-dibenzyloxypyridine (9)

Compound **8** (2 g, 6.25 mmol) was dissolved in acetone (20 mL) and water (20 mL). To this solution was added sulfamic acid (850 mg, 8.75 mmol, 1.4 equiv) and sodium chlorite (80%, 622 mg, 6.87 mmol, 1.1 equiv) and stirred at room temperature for 3 h. in an open flask. Removal of acetone in vacuo yielded crude product as a precipitate in the remaining aqueous solution. This was collected, washed with acetone and dried to yield off-white powder, mp 120 °C. Yield 77%. ν_{max} (KBr) 3033 (br, O–H), 1707 (br, acid C=O), 1607 and 1499 (ring C=C), 1223 and 1026 (C–O–C) cm^{-1}. ^1H NMR (MeOD) δ 5.15 (2H, s, 3-OCH_2Ph), 5.39 (2H, s, 4-OCH_2Ph), 7.25–7.55 (10, m, 3-OCH$_2$*Ph* and 4-OCH$_2$*Ph*), 7.55 (1H, d, J = 6.2 Hz, 5-*H*), 8.32 (1H, d, J = 6.2 Hz, 6-*H*); *m*/*z* (ESI): 334.8.

4.1.9. General procedure for preparation of compounds 10e,f,i

This procedure is illustrated for compound **10e**. To a solution of *Z*-glycine (550 mg, 2.4 mmol) in dry dichloromethane (10 mL) at 0 °C and under nitrogen, *N*-(dimethylaminopropyl)-*N*-ethylcarbodiimide hydrochloride (EDC) (690 mg, 3.6 mmol, 1.5 equiv), TEA (364 mg, 3.6 mmol, 1.5 equiv), DMAP (293 mg, 2.4 mmol, 1 equiv) were added. The mixture was allowed to stir for 10 min before benzylamine (1.03 g, 9.6 mmol, 4 equiv) was added, and the reaction was left to stir at room temperature for 12 h. Then, the mixture was concentrated under reduced pressure, and the residue was diluted with ethyl acetate, washed sequentially with 5% citric acid solution (2×), saturated aqueous sodium bicarbonate (2×), and brine, dried over anhydrous Na_2SO_4 and concentrated under reduced pressure, to afford the title compound as a white solid. Yield 85%. ^1H NMR ($CDCl_3$) δ 3.90 (d, 2H, J = 5.6 Hz, αCH_2), 4.45 (d, 2H, J = 5.8 Hz, NHCH_2-Ph), 5.11 (s, 2H, cbzCH_2), 5.36 (br s, 1H, N*H*CH$_2$Ph) 6.24 (br s, 1H, N*H*cbz), 7.34 (m, 10H, cbz*Ph* and NHCH$_2$*Ph*); *m*/*z* (ESI): 298.1.

Compound **10f**: Yield 57%. ^1H NMR ($CDCl_3$) δ 1.41 (d, 3H, J = 7.0 Hz, αCHCH_3). 4.25 (m, 1H, αC*H*CH$_3$), 4.44 (m, 2H, NHCH_2-Ph), 5.09 (s, 2H, cbzCH_2), 5.28 (br s, 1H, N*H*CH$_2$Ph) 6.32 (br s, 1H, N*H*cbz), 7.26–7.34 (m, 10H, cbz*Ph* and NHCH$_2$*Ph*); *m*/*z* (ESI): 311.8.

Compound **10i**: Yield 92.8%. ^1H NMR ($CDCl_3$) δ 3.09 (2dd, 2H, J = 6.2 Hz, 7.6 Hz, αCHCH_2Ph), 4.33 (m, 1H, αC*H*CH$_2$Ph), 4.45 (m, 2H, NHCH_2-Ph), 5.03 (s, 2H, cbzCH_2), 5.45 (br s, 1H, N*H*CH$_2$Ph) 6.22 (br s, 1H, N*H*cbz), 7.06–7.34 (m, 15H, cbz*Ph*, αCHCH$_2$*Ph* and NHCH$_2$*Ph*); *m*/*z* (ESI): 388.0.

4.1.10. General procedure for preparation of compounds 10a,b,c,d,e,h,j,k

This procedure is illustrated for compound **10a**. To a stirred solution of *Z*-glycine (250 mg, 1.2 mmol) in dichloromethane at 0 °C, dicyclohexylcarbodiimide (DCC) (296 mg, 1.44 mmol, 1.2 equiv) and hydroxybenzotriazole (HOBt) (195 mg, 1.44 mmol, 1.2 equiv) were added. The reaction mixture was maintained at 0 °C for 1 h, and then it was allowed to warm up to room temperature. The methylamine (112 mg, 3.6 mmol, 3 equiv) was added, and the reaction mixture was stirred for 12 h. The DCU was filtered, and the organic layer was washed with 5% citric acid solution (2×), saturated aqueous sodium bicarbonate (2×), and brine, dried and concentrated in vacuo, to afford a clear oil. The obtained residue was purified by flash column chromatography (EtOAc/hexane, 8:2), affording the title compound as a white solid. Yield 64%. ^1H NMR ($CDCl_3$) δ 2.80 (d, 3H, J = 4.8 Hz, CH_3NH–), 3.84 (d, 2H, J = 5.8 Hz, αCH_2), 5.12 (s, 2H, cbzCH_2), 5.43 (br s, 1H, N*H*CH$_3$) 6.04 (br s, 1H, N*H*cbz), 7.35 (m, 5H, cbz*Ph*); *m*/*z* (ESI): 221.8.

Compound **10b**: Yield 63%. ^1H NMR ($CDCl_3$) δ 0.88 (d, 6H, J = 6.7 Hz, –CH$_2$CH(CH_3)$_2$), 1.75 (m, 1H, J = 6.4 Hz, 6.7 Hz, –CH$_2$C*H*(CH$_3$)$_2$), 3.08 (t, 2H, J = 6.4 Hz, –CH_2CH(CH$_3$)$_2$), 3.85 (d, 2H, J = 5.7 Hz, αCH_2), 5.13 (s, 2H, cbzCH_2), 5.47 (br s, 1H, N*H*CH$_2$CH(CH$_3$)$_2$) 6.09 (br s, 1H, N*H*cbz), 7.35 (m, 5H, cbz*Ph*); *m*/*z* (ESI): 263.9.

Compound **10c**: Yield 75.6%. ^1H NMR ($CDCl_3$) δ 1.36 (d, 3H, J = 7.1 Hz, αCHCH_3), 2.78 (d, 3H, J = 4.8 Hz, CH_3NH-), 4.21 (m, 1H, αC*H*CH$_3$), 5.18 (s, 2H, cbzCH_2), 5.49 (br s, 1H, N*H*CH$_3$) 6.33 (br s, 1H, N*H*cbz), 7.33 (m, 5H, cbz*Ph*); *m*/*z* (ESI): 235.7.

Compound **10d**: Yield 80%. ^1H NMR ($CDCl_3$) δ 0.88 (d, 6H, J = 6.7 Hz, –CH$_2$CH(CH_3)$_2$), 1.38 (d, 3H, J = 6.9 Hz, αCHCH_3), 1.75 (m, 1H, J = 6.7 Hz, –CH$_2$C*H*(CH$_3$)$_2$), 3.06 (m, 2H, CH_2CH(CH$_3$)$_2$), 4.20 (m, 1H, αC*H*CH$_3$), 5.10 (s, 2H, cbzCH_2), 5.36 (br s, 1H, N*H*cbz) 6.13 (br s, 1H, N*H*CH$_2$CH(CH$_3$)$_2$), 7.34 (m, 5H, cbz*Ph*); *m*/*z* (ESI): 278.3.

Compound **10g**: Yield 85%. ^1H NMR ($CDCl_3$) δ 2.71 (d, 3H, J = 4.8 Hz, –NHCH_3), 3.02 (dd, 1H, J_{gem}=13.6 Hz, J_{vic} = 7.6 Hz, –αCHCH_2Ph), 3.12 (dd, 1H, J_{gem} = 13.6 Hz, J_{vic} = 6.0 Hz, -αCHCH_2Ph), 4.30–4.36 (m, 1H, –αC*H*CH$_2$Ph), 5.08 (s, 2H, cbzCH_2), 5.32 (br s, 1H, N*H*cbz) 5.61 (br s, 1H, N*H*CH$_3$), 7.17–7.38 (m, 10H, cbz*Ph* and -αCHCH$_2$*Ph*); *m*/*z* (ESI): 311.7.

Compound **10h**: Yield 78%. ^1H NMR ($CDCl_3$) δ 0.74 (d, 3H, J = 6.5 Hz, –CH$_2$CH(CH_3)$_2$), 0.76 (d, 3H, J = 6.4 Hz, -CH$_2$CH(CH_3)$_2$), 1.53–1.64 (m, 1H, –CH$_2$C*H*(CH$_3$)$_2$), 2.94–2.98 (m, 2H, -CH_2CH(CH$_3$)$_2$), 3.02 (dd, 1H, J_{gem} = 13.6 Hz, J_{vic} = 7.8 Hz, –αCHCH_2Ph), 3.12 (dd, 1H, J_{gem} = 13.6 Hz, J_{vic} = 6.2 Hz, –αCHCH_2Ph), 4.32–4.38 (m, 1H, –αC*H*CH$_2$Ph), 5.08 (s, 2H, cbzCH_2), 5.39 (br s, 1H, N*H*cbz) 5.68 (br s, 1H, –N*H*CH$_2$CH(CH$_3$)$_2$), 7.18–7.35 (m, 10H, cbz*Ph* and -αCHCH$_2$*Ph*); *m*/*z* (ESI): 353.9.

Compound **10j**: Yield 77%. ^1H NMR ($CDCl_3$) δ 2.96 (s, 3H, N(CH_3)$_2$), 2.98 (s, 3H, N(CH_3)$_2$), 4.00 (d, 2H, J = 4.2 Hz, –αCH_2–), 5.12 (s, 2H, cbzCH_2), 5.83 (br s, 1H, N*H*cbz), 7.30–7.41 (m, 5H, cbz*Ph*); *m*/*z* (ESI): 237.2.

Compound **10k**: Yield 82%. ^1H NMR ($CDCl_3$) δ 1.51–1.70 (m, 6H, pip), 3.30 (t, 2H, J = 5.4 Hz, -pip), 3.56 (t, 2H, J = 5.5 Hz, pip), 4.00 (d, 2H, J = 4.2 Hz, –αCH_2–), 5.12 (s, 2H, cbzCH_2), 5.87 (br s, 1H, N*H*cbz), 7.30–7.36 (m, 5H, cbz*Ph*); *m*/*z* (ESI): 275.8.

4.1.11. General procedure for preparation of compounds 11a–k

This procedure is illustrated for compound **11a**. To a solution of compound **10a** (170 mg, 0.77 mmol) in methanol (10 mL), 10% Pd/C was added. The reaction was hydrogenated at room temperature and atmospheric pressure for 3 h. Then the catalyst was filtered off through Celite, and the clear solution, taken to dryness, afforded the title compound as an oil. The reaction was monitored by TLC and, for stability problems, the amine was directly used in the subsequent reaction. Yield 97%.

Compound **11b**: The reaction was monitored by TLC and, for stability problems, the amine was directly used in the subsequent reaction. Yield 94%.

Compound **11c**: The reaction was monitored by TLC and, for stability problems, the amine was directly used in the subsequent reaction. Yield 96%.

Compound **11d**: The reaction was monitored by TLC and, for stability problems, the amine was directly used in the subsequent reaction. Yield 97%.

Compound **11e**: Yield 96%. ^1H NMR (CD_3OD) δ 3.73 (s, 2H, –CH_2NH$_2$), 4.44 (s, 2H, –NHCH_2Ph), 7.25–7.46 (m, 5H, –NHCH$_2$*Ph*).

Compound **11f**: Yield 97%. ^1H NMR (CD_3OD) δ 1.30 (d, 3H, J = 6.9 Hz, –CH(CH_3)NH$_2$), 3.44–3.50 (m, 1H, -C*H*(CH$_3$)NH$_2$), 4.36 (s, 2H, –NHCH_2Ph), 7.23–7.35 (m, 5H, –NHCH$_2$*Ph*).

Compound **11g**: Yield 96%. ^1H NMR ($CDCl_3$) δ 2.65 (dd, 1H, J_{gem} = 13.7 Hz, J_{vic} = 9.4 Hz, -αCHCH_2Ph), 2.80 (d, 3H, J = 4.9 Hz, –NHCH_3), 3.27 (dd, 1H, J_{gem} = 13.7 Hz, J_{vic} = 3.9 Hz, –αCHCH_2Ph),

3.59 (dd, 1H, J = 3.9, 9.4 Hz, –αC*H*CH$_2$Ph), 7.08–7.44 (m, 5H, –αCHCH$_2$*Ph*).

Compound **11h**: Yield 94%. ^{1}H NMR (CDCl$_3$) δ 0.89 (d, 6H, J = 5.2 Hz, (C*H*$_3$)$_2$CHCH$_2$NH–), 1.70–1.76 (m, 1H, (CH$_3$)$_2$C*H*CH$_2$NH–), 2.69 (dd, 1H, J_{gem} = 13.7 Hz, J_{vic} = 9.2 Hz, –αCHC*H*$_2$Ph), 3.05–3.10 (m, 2H, (CH$_3$)$_2$CHC*H*$_2$NH–), 3.26 (dd, 1H, J_{gem} = 13.7 Hz, J_{vic} = 4.0 Hz, –αCHC*H*$_2$Ph), 3.60 (dd, 1H, J = 4.0, 9.2 Hz, -α*CH*CH$_2$Ph), 7.20–7.37 (m, 5H, –αCHCH$_2$*Ph*).

Compound **11i**: Yield 95%. ^{1}H NMR (CDCl$_3$) δ 3.03 (2H, m, αCHC*H*$_2$Ph), 3.96 (1H, t, J = 7.1 Hz, α*CH*CH$_2$Ph), 4.25 (2H, dd, J = 14.3 Hz, NHC*H*$_2$Ph), 7.03–7.34 (10H, m, NHCH$_2$*Ph* and αCHCH$_2$*Ph*).

Compound **11j**: The reaction was monitored by TLC and, for stability problems, the amine was directly used in the subsequent reaction. Yield 94%.

Compound **11k**: The reaction was monitored by TLC and, for stability problems, the amine was directly used in the subsequent reaction. Yield 97%.

4.1.12. General procedure for preparation of compounds 12a–k

This procedure is illustrated for compound **12a**. To a stirred solution of **9** (287 mg, 0.85 mmol) in dichloromethane at 0 °C, dicyclohexylcarbodiimide (DCC) (211 mg, 1.02 mmol, 1.2 equiv) and hydroxybenzotriazole (HOBt) (138 mg, 1.02 mmol, 1.2 equiv) were added. The reaction mixture was maintained at 0 °C for 1 h, and then it was allowed to warm up to room temperature. Compound **11a** (130 mg, 1.27 mmol, 1.5 equiv) was added, and the reaction mixture was stirred for 12 h. The DCU was filtered, and the organic layer was washed with 5% citric acid solution (2×), saturated aqueous sodium bicarbonate (2×), and brine, dried and concentrated in vacuo, to afford a clear oil. The obtained residue was purified by flash column chromatography (chloroform/methanol, 9:1), affording the title compound as a white solid. Yield 75.6%. ^{1}H NMR (CDCl$_3$) δ 2.77 (d, 3H, J = 4.9 Hz, NHC*H*$_3$), 4.06 (d, 2H, J = 6.1 Hz, αC*H*$_2$), 5.14 (s, 2H, 3-OC*H*$_2$Ph), 5.18 (s, 2H, 4-OC*H*$_2$Ph), 6.39 (br s, 1H), 7.01 (d, 1H, J = 5.4 Hz, 5-*H*), 7.28–7.45 (m, 10H, 3-OCH$_2$*Ph* and 4-OCH$_2$*Ph*), 8.22 (d, 1H, J = 5.4 Hz, 6-*H*); m/z (ESI): 405.3.

Compound **12b**: Yield 45%. ^{1}H NMR (CDCl$_3$) δ 0.87 (d, 6H, J = 6.7 Hz, CH$_2$CH(C*H*$_3$)$_2$) 1.75 (m, 1H, J = 6.7 Hz, CH$_2$C*H*(CH$_3$)$_2$), 3.06 (t, 2H, J = 6.6 Hz, C*H*$_2$CH(CH$_3$)$_2$), 4.07 (d, 2H, J = 5.9 Hz, αC*H*$_2$), 5.14 (s, 2H, 3-OC*H*$_2$Ph), 5.18 (s, 2H, 4-OC*H*$_2$Ph), 6.48 (br s, 1H), 7.01 (d, 1H, J = 5.4 Hz, 5-*H*), 7.28–7.45 (m, 10H, 3-OCH$_2$*Ph* and 4-OCH$_2$*Ph*), 8.23 (d, 1H, J = 5.4 Hz, 6-*H*), 8.25 (m, 1H); m/z (ESI): 446.7.

Compound **12c**: Yield 75.6%. ^{1}H NMR (CDCl$_3$) δ 1.40 (d, 3H, J = 7.1 Hz, –αCHC*H*$_3$), 2.76 (d, 3H, J = 4.8 Hz, –NHC*H*$_3$), 4.65 (q, 1H, J = 7.1 Hz, –αC*H*CH$_3$), 5.12–5.18 (m, 4H, 3-OC*H*$_2$Ph and 4-OC*H*$_2$Ph), 6.54 (br s, 1H, -N*H*CH$_3$), 7.01 (d, 1H, J = 5.4 Hz, 5-*H*), 7.29–7.45 (m, 10H, 3-OCH$_2$*Ph* and 4-OCH$_2$*Ph*), 8.06 (br s, 1H, –CON*H*–), 8.24 (d, 1H, J = 5.4 Hz, 6-*H*); m/z (ESI): 419.0.

Compound **12d**: Yield 60%. ^{1}H NMR (CDCl$_3$) δ 0.85 (d, 6H, J = 6.7 Hz, –CH$_2$CH(C*H*$_3$)$_2$), 1.42 (d, 3H, J = 7.1 Hz, –αCHC*H*$_3$), 1.69–1.79 (m, 1H, –CH$_2$C*H*(CH$_3$)$_2$), 3.04 (m, 2H, –C*H*$_2$CH(CH$_3$)$_2$), 4.67 (q, 1H, J = 7.1 Hz, –αC*H*CH$_3$), 5.12–5.16 (m, 4H, 3-OC*H*$_2$Ph and 4-OC*H*$_2$Ph), 6.72 (br s, 1H, –N*H*CH$_2$CH(CH$_3$)$_2$), 6.99 (d, 1H, J = 5.4 Hz, 5-*H*), 7.27–7.45 (m, 10H, 3-OCH$_2$*Ph* and 4-OCH$_2$*Ph*), 8.13 (br s, 1H, –CON*H*–), 8.22 (d, 1H, J = 5.4 Hz, 6-*H*); m/z (ESI): 461.4.

Compound **12e**: Yield 55.3%. ^{1}H NMR (CDCl$_3$) δ 4.02 (d, 2H, J = 5.4 Hz, αC*H*$_2$), 4.33 (d, 2H, J = 5.8 Hz, NHC*H*$_2$Ph), 5.04 (s, 2H, 3-OC*H*$_2$Ph), 5.06 (s, 2H, 4-OC*H*$_2$Ph), 6.88 (d, 1H, J = 5.3 Hz, 5-*H*), 7.13–7.37 (m, 16H, 3-OCH$_2$*Ph*, 4-OCH$_2$*Ph*, N*H*), 8.09 (d, 1H, J = 5.3 Hz, 6-*H*), 8.36 (t, 1H, J = 5.4 Hz, N*H*); m/z (ESI): 481.0.

Compound **12f**: Yield 48.4%. ^{1}H NMR (CDCl$_3$) δ 1.43 (d, 3H, J = 6.9 Hz, –αCHC*H*$_3$), 4.34–4.44 (m, 2H, –NHC*H*$_2$Ph), 4.68–4.76 (m, 1H, –αC*H*CH$_3$), 5.03–5.11 (m,2H, 3-OC*H*$_2$Ph), 5.15 (s, 2H, 4-OC*H*$_2$Ph), 6.97 (d, 1H, J = 5.3 Hz, 5-*H*), 7.08 (br s, 1H, -N*H*Bn), 7.17–7.41 (m, 15H, 3-OCH$_2$*Ph*, 4-OCH$_2$*Ph* and –NHCH$_2$*Ph*), 8.17 (br s, 1H, –CON*H*–), 8.19 (d, 1H, J = 5.3 Hz, 6-*H*); m/z (ESI): 495.1.

Compound **12g**: Yield 31.2%. ^{1}H NMR (CDCl$_3$) δ 2.65 (d, 3H, J = 4.7 Hz, NHC*H*$_3$), 3.04–3.16 (m, 2H, –C*H*$_2$Ph), 4.82–4.88 (m, 1H, –αC*H*CH$_2$Ph), 5.01–5.05 (m, 2H, 3-OC*H*$_2$Ph), 5.14 (s, 2H, 4-OC*H*$_2$Ph), 6.45 (br s, 1H, –N*H*CH$_3$), 6.96 (d, 1H, J = 5.1 Hz, 5-*H*), 7.15–7.44 (m, 15H, 3-OCH$_2$*Ph*, 4-OCH$_2$*Ph* and –CH$_2$*Ph*), 8.19 (d, 1H, J = 5.1 Hz, 6-*H*), 8.35 (d, 1H, J = 7.9 Hz, –CON*H*–); m/z (ESI): 494.8.

Compound **12h**: Yield 43%. ^{1}H NMR (CDCl$_3$) δ 0.73–0.76 (m, 6H, –CH$_2$CH(C*H*$_3$)$_2$), 1.57–1.65 (m, 1H, -CH$_2$C*H*(CH$_3$)$_2$), 2.93–2.99 (m, 2H, –C*H*$_2$CH(CH$_3$)$_2$), 3.06–3.19 (m, 2H, –C*H*$_2$Ph), 4.81–4.83 (m, 1H, –αC*H*CH$_2$Ph), 5.09 (s, 2H, 3-OC*H*$_2$Ph), 5.18 (s, 2H, 4-OC*H*$_2$Ph), 6.21 (br s, 1H, –N*H*CH$_2$CH(CH$_3$)$_2$), 6.97–6.98 (m, 1H, 5-*H*), 7.18–7.69 (m, 15H, 3-OCH$_2$*Ph*, 4-OCH$_2$*Ph* and –CH$_2$*Ph*), 8.19 (m, 1H, 6-*H*), 8.28 (d, 1H, J = 5.7 Hz, –CON*H*–); m/z (ESI): 536.9.

Compound **12i**: Yield 54.5%. ^{1}H NMR (CDCl$_3$) δ 3.16 (d, 2H, J = 7.2 Hz, –C*H*$_2$Ph), 4.27–4.39 (m, 2H, –NHC*H*$_2$Ph), 4.87 (q, 1H, J = 7.2 Hz, 8.1 Hz, –αC*H*CH$_2$Ph), 5.05 (s, 2H, 3-OC*H*$_2$Ph), 5.15 (s, 2H, 4-OC*H*$_2$Ph), 6.43 (br s, 1H), 6.97 (d, 1H, J = 5.4 Hz, 5-*H*), 7.05–7.07 (m, 1H), 7.18–7.27 (m, 15H), 7.33–7.42 (m, 4H), 8.18 (d, 1H, J = 5.4 Hz, 6-*H*), 8.30 (d, 1H, J = 8.1 Hz, –CON*H*–); m/z (ESI): 571.4.

Compound **12j**: Yield 57.3%. ^{1}H NMR (CDCl$_3$) δ 3.01 (s, 3H, NH(C*H*$_3$)$_2$), 3.02 (s, 3H, NH(C*H*$_3$)$_2$), 4.23 (d, 2H, J = 4.2 Hz, αC*H*$_2$), 5.16 (s, 2H, 3-OC*H*$_2$Ph), 5.17 (s, 2H, 4-OC*H*$_2$Ph), 6.98 (d, 1H, J = 5.3 Hz, 5-*H*), 7.37–7.47 (m, 10H, 3-OCH$_2$*Ph* and 4-OCH$_2$*Ph*), 8.25 (d, 1H, J = 5.3 Hz, 6-*H*), 8.56 (br s, 1H, –CON*H*–); m/z (ESI): 419.7.

Compound **12k**: Yield 75.6%. ^{1}H NMR (CDCl$_3$) δ 1.51–1.67 (m, 6H, pip), 3.38 (t, 2H, J = 5.4 Hz, pip), 3.60 (t, 2H, J = 5.5 Hz, pip), 4.22 (d, 2H, J = 4.2 Hz, αC*H*$_2$), 5.16 (s, 2H, 3-OC*H*$_2$Ph), 5.17 (s, 2H, 4-OC*H*$_2$Ph), 6.98 (d, 1H, J = 5.4 Hz, 5-*H*), 7.36–7.70 (m, 10H, 3-OCH$_2$*Ph* and 4-OCH$_2$*Ph*), 8.25 (d, 1H, J = 5.3 Hz, 6-*H*), 8.59 (br s, 1H, -CON*H*-); m/z (ESI): 459.1.

4.1.13. Preparation of compound 14

A solution of **12a** in methyl iodide is stirred overnight under reflux condition. After cooling, ethyl acetate is added to the mixture. The white precipitate formed is filtered off the solution and recrystallised from methanol/diethylether to afford **14** as white crystals. Yield 92.5%. ^{1}H NMR (CD$_3$OD) δ 2.75 (s, 3H, NHC*H*$_3$), 4.04 (s, 2H, αC*H*$_2$), 4.26 (s, 3H, RN$^+$–C*H*$_3$I$^-$),5.18 (s, 2H, 3-OC*H*$_2$Ph), 5.58 (s, 2H, 4-OC*H*$_2$Ph), 7.29–7.59 (m, 10H, 3-OCH$_2$*Ph* and 4-OCH$_2$*Ph*), 7.85 (d, 1H, J = 7.2 Hz, 5-*H*), 8.67 (d, 1H, J = 7.1 Hz, 6-*H*); m/z (ESI): 420.3.

4.1.14. General procedure for preparation of compounds 13a–k and 15

This procedure is illustrated for compound **13a**. A solution of **12a** (270 mg, 0.643 mmol) in dry dichloromethane (mL) was cooled to 0 °C before BCl_3 (1 M dichloromethane solution, 2 mL, 1.97 mmol, 3 equiv) was slowly added. The reaction mixture was left under stirring for 3 h. Then, methanol was slowly added, and the solution was concentrated in vacuo. The following crystallisation from methanol/acetone afforded the desired compound in the HCl salt form as a white amorphous powder. Yield 96%. ^{1}H NMR (CD$_3$OD) δ 2.79 (s, 3H, –NHC*H*$_3$), 4.18 (s, 2H,-NHC*H*$_2$CO-), 7.37 (d, 1H, J = 6.4 Hz, 5-*H*), 8.21 (d, 1H, J = 6.4 Hz, 6-*H*); m/z (ESI): 226.00, 194.98, 167.07, 156.00.

Compound **13b**: Yield 93%. ^{1}H NMR (CD$_3$OD) δ 0.94 (d, 6H, J = 6.7 Hz, –CH$_2$CH(C*H*$_3$)$_2$), 1.82 (m, 1H, J = 6.7, 6.9 Hz, -CH$_2$C*H*(CH$_3$)$_2$), 3.07 (d, 2H, J = 6.9 Hz, –C*H*$_2$CH(CH$_3$)$_2$), 4.21 (s, 2H, –NHC*H*$_2$CO–), 7.34 (d, 1H, J = 6.4 Hz, 5-*H*), 8.18 (d, 1H, J = 6.4 Hz, 6-*H*); m/z (ESI): 268.07, 195.00, 167.07.

Compound **13c**: Yield 96.5%. ^{1}H NMR (CD_3OD) δ 1.50 (d, 3H, J = 6.9 Hz, –αCH(CH_3)), 2.79 (s, 3H, -NHCH_3), 4.64 (q, 1H, J = 6.9 Hz, –NHCH(CH_3)CO), 7.37 (d, 1H, J = 6.4 Hz, 5-H), 8.20 (d, 1H, J = 6.4 Hz, 6-H); m/z (ESI): 240.07, 209.00, 181.07, 156.07.

Compound **13d**: Yield 96%. ^{1}H NMR (CD_3OD) δ 0.94 (d, 6H, J = 6.7 Hz, –CH_2CH(CH_3)$_2$), 1.52 (d, 3H, J = 6.9 Hz, –αCHCH_3), 1.82 (m, 1H, J = 6.7, 6.9 Hz, -CH_2CH(CH_3)$_2$), 3.07 (d, 2H, J = 6.9 Hz, –CH_2CH(CH_3)$_2$), 4.63–4.69 (m, 1H, –αCHCH$_3$), 7.30 (d, 1H, J = 6.2 Hz, 5-H), 8.16 (d, 1H, J = 6.2 Hz, 6-H); m/z (ESI): 282.07, 209.00, 181.00, 156.07.

Compound **13e**: Yield 95%. ^{1}H NMR (CD_3OD) δ 4.23 (s, 2H, –NHCH_2CO–), 4.42 (s, 2H, -NHCH_2Ph), 7.29–7.34 (m, 6H, –NHCH$_2$*Ph*), 8.17 (d, 1H, J = 6.4 Hz, 6-H); m/z (ESI): 302.40, 195.03, 167.07, 156.07.

Compound **13f**: Yield 98%. ^{1}H NMR (CD_3OD) δ 1.43 (d, 3H, J = 7.0 Hz, –αCHCH_3), 4.32 (s, 2H, –NHCH_2Ph), 4.59 (q, 1H, J = 7.0 Hz, –αCHCH$_3$), 7.11–7.43 (m, 6H, -CH_2*Ph* and 5-H), 8.06 (d, 1H, J = 6.4 Hz, 6-H); m/z (ESI): 316.17, 208.94, 181.00, 156.00.

Compound **13g**: Yield 97.5%. ^{1}H NMR (CD_3OD) δ 2.72 (s, 3H, -NHCH_3), 3.14 (dd, 1H, J_{gem} = 13.7 Hz, J_{vic} = 7.2 Hz, -CH_2Ph), 3.22 (dd, 1H, J_{gem} = 13.7 Hz, J_{vic} = 6.1 Hz, -CH_2Ph), 4.84 (t, 1H, J = 6.9 Hz, –αCHCH$_2$Ph), 7.22–7.33 (m, 6H, -CH_2*Ph* and 5-H), 8.15 (d, 1H, J = 6.4 Hz, 6-H); m/z (ESI): 316.07, 284.98, 257.04, 120.06.

Compound **13h**: Yield 96.5%. ^{1}H NMR (CD_3OD) δ 0.73 (d, 3H, J = 5.1 Hz, –CH_2CH(CH_3)$_2$), 0.74 (d, 3H, J = 5.1 Hz, –CH_2CH(CH_3)$_2$), 1.56–1.67 (m, 1H, –CH_2CH(CH_3)$_2$), 2.83 (dd, 1H, J_{gem} = 13.2 Hz, J_{vic} = 7.1 Hz, –CH_2Ph), 3.93 (dd, 1H, J_{gem} = 13.2 Hz, J_{vic} = 6.8 Hz, –CH_2Ph), 3.00–3.12 (m, 2H, –CH_2CH(CH_3)$_2$), 4.77 (t, 1H, J = 6.9 Hz, -αCHCH$_2$Ph), 7.11–7.22 (m, 4H), 7.45–7.57 (m, 2H), 8.05 (d, 1H, J = 6.4 Hz, 6-H); m/z (ESI): 358.13, 285.00, 257.07, 120.07.

Compound **13i**: Yield 97%. ^{1}H NMR (CD_3OD) δ 3.13–3.25 (m, 2H, αCHCH_2Ph), 4.37 (dd, 2H, J = 14.9 Hz, –NHCH_2Ph), 4.85 (m, 1H, αCHCH$_2$Ph), 7.07 (d, 1H, J = 6.4 Hz, 5-H), 7.18–7.31 (m, 10H, -αCHCH$_2$*Ph* and -NHCH$_2$*Ph*), 7.98 (d, 1H, J = 6.4 Hz, 6-H); m/z (ESI): 392.13, 285.02, 257.07, 120.07, 103.07.

Compound **13j**: Yield 96%. ^{1}H NMR (CD_3OD) δ 3.02 (s, 3H, –N(CH_3)$_2$), 3.10 (s, 3H, -N(CH_3)$_2$), 4.41 (s, 2H,-NHCH_2CO-), 7.33 (d, 1H, J = 6.4 Hz, 5-H), 8.18 (d, 1H, J = 6.4 Hz, 6-H)); m/z (ESI): 239.2.

Compound **13k**: Yield 97%. ^{1}H NMR (CD_3OD) δ 1.60–1.73 (m, 6H, pip), 3.49 (t, 2H, J = 5.2 Hz, pip), 3.61 (t, 2H, J = 5.5 Hz, pip), 4.41 (s, 2H,-NHCH_2CO-), 7.30 (d, 1H, J = 6.2 Hz, 5-H), 8.15 (d, 1H, J = 6.3 Hz, 6-H)); m/z (ESI): 278.9.

Compound **15:** Yield 96%. ^{1}H NMR (CD_3OD) δ 2.81 (s, 3H, -NHCH_3), 4.11 (s, 2H,-NHCH_2CO-), 4.15 (s, 3H,-RNCH_3) 7.22 (d, 1H, J = 6.8 Hz, 5-H), 8.23 (d, 1H, J = 6.8 Hz, 6-H)); m/z (ESI): 240.7.

4.2. Crystallography

Single crystal X-ray diffraction data of **13f** was collected on a BRUKER AXS SMART 6000 diffraction system at 293 K using Cu Kα radiation (λ = 1.54178 Å). The structure was solved by direct methods using the program system SHELXS 97 [X]. All non-hydrogen atoms were taken from a series of full-matrix least-squares refinement cycles based on F^2 using the program SHELXL 97) followed by difference Fourier syntheses. All hydrogen atoms were placed on calculated positions and were allowed to ride on their corresponding carbon atoms. The isotropic thermal parameters for the methyl protons were set to 1.5 times and for all other hydrogen atoms to 1.2 times of the U_{eq} value of the bonding atom. All non-hydrogen atoms were refined anisotropically. Experimental details of the X-ray diffraction studies are listed in Table 3. CCDC676400 contains the supplementary crystallographic data for this paper. This data can be obtained free of charge via http://www.ccdc.cam.ac.uk/conts/retrieving.html or from the CCDC, 12 Union Road, Cambridge CB2 1EZ, UK; fax: +44 1223 336033; email: deposit@ccdc.cam.ac.uk.

4.3. Log *D* Determination and log *P* Estimation by HPLC

The log D values of compounds **13 a–l** were determined by the shake-flask method using n-octanol-aqueous buffer at 25 °C. A HPLC method was also adopted. *Shake-flask method*. The lipophicility, expressed as distribution coefficient at physiological pH 7.4, was measured using n-octanol and MOPS (3-N-morpholinopropanesulfonic acid 0.1 mM) buffer. The absorbance of a solution of known concentration (0.1 mM) of the test compound in the buffer was recorded spectrophotometrically (A_{289}). A given volume (5 mL) of this solution was then shaken with the same volume of n-octanol by vigorous stirring for 1 h. The two layers were separated by centrifugation and the absorbance of the aqueous phase was measured again. The decrease in absorbance of the aqueous phase, due to partitionon into the organic phase, indicated the lipophicility, which was then calculated and expressed as log D from the ratio of the drug concentration in n-octanol and the drug concentration in the MOPS buffer, using the following equation:

$$D = [\text{Drug}]_{\text{buffer}}/[\text{Drug}]_{\text{octanol}}$$

$[\text{Drug}]_{\text{buffer}} = A_1/A_0 \times 0.1$ and $[\text{Drug}]_{\text{octanol}} = 0.1 - [\text{Drug}]_{\text{buffer}}$, where A_0 is the initial absorbance of the aqueous phase and A_1 is the absorbance of the aqueous phase after partition with n-octanol.

HPLC method. A Hewlet-Packard model 1090 M Series HPLC system with an autoinjector, autosampler, diode array detector and a reverse phase polymer HPLC column (PLRP-S 100 Å, 23 × 0.46 cm, 5 μm) was used in the study. The mobile phase consisted of ion pair buffer (5 mM 1-heptanesulfonic acid, sodium salt; pH adjusted to 2 using HCl), which was chosen to minimise any effect derived from the ionisation state of the analysed compounds, and acetonitrile. The gradient used was 2–35% acetonitrile in 20 min, the flow rate was 1 ml/min and the analytes were e monitored at 280 nm. Each sample was run in triplicate. The partition coefficient was calculated from retention data by regression analysis using a small library of previously studied HPOs as standards.[33]

4.4. Ligand pK_a values and stability constant of iron(III) complexes

Iron chloride (17.906 mM in 1% HCl, atomic absorption standard, Aldrich) was utilized in this study. Analytical grade reagent HCl (37%) and KOH (10 M) ampoules (Fisher), HPLC grade water and methanol (Fisher) were used in the preparation of all solutions. The automatic titration system used in this study comprises of an autoburette (Metrohm Dosimat 765, l mL syringe) and Mettler Toledo MP230 pH meter with Metrohm AgCl electrode (6.0133.100) and a reference electrode (6.0733.100). 0.1 M KCl electrolyte solution was used to maintain the ionic strength. The temperature of the test solutions was maintained at 25 ± 0.1 °C by a Techne TE-8 J temperature controller. The solution under investigation was stirred vigorously. A Gilson mini-plus3 pump with speed capability (20 mL/min) was used to circulate the test solution into a Hellem quartz flow cuvette. For stability constant determinations a 50 mm path length cuvette was used and for pK_a determinations a cuvette path length of 10 mm was used. Automatic titration and spectral scans adopted the following strategy: increase or decrease the pH value of the solution by 0.1 pH unit by the addition of KOH or HCl from the autoburette. When pH readings varied by <0.001 pH unit over a 3 s period, the solution was allowed to reach equilibrium (for stability constant determinations a period of 5 minutes was adopted, for pK_a determinations a period of 1 minute was adopted). The spectrum of the solution was then recorded. The cycle was then repeated automatically until the defined end point pH value was achieved. Following electrode calibration, samples with an appropriate concentration to give measurable absorbance were titrated in pH range 2–12

for pK_a determination. For affinity studies, iron ligand ratio was kept at 5:1. Insoluble iron(III) complexes were measured in 1:1 methanol/water mixtures, the results were converted to those corresponding to aqueous conditions. The titration data were analyzed by pHab.[34,35]

Affinity is expressed as pM value pM is defined as the negative logarithm of the metal ion concentration under the following conditions: $[\text{Metal Ion}]_{total} = 10^{-6}$ M, $[\text{Ligand}]_{total} = 10^{-5}$ M at pH 7.4.

4.5. Lipoxygenase and tyrosine hydroxylase inhibition

Lipoxygenase. Isolated soybean lipoxygenase (sbLPO) and its preferential substrate linoleic acid were both purchased from Sigma. The inhibition of the enzyme was monitored by a change in the absorption of the product linoleic hydroperoxide at 234 nm. The enzyme (1 μM solution in borate buffer 0.2 M, pH 9) was pre-incubated with the test compound (100 μM, final concentration in the cuvette of 10 μM)) for 15 min, and the reaction was initiated by the addition of linoleic acid (1 mM). The reaction was monitored at 234 nm for 10 min using a time based measurement. The rates of reactions were determined using the molar absorption coefficient of hydroperoxide ($\varepsilon = 23600\ M^{-1}\ cm^{-1}$). None of the synthesised compounds showed inhibitory activity at 10 μM. *Tyrosine hydroxylase.* Rat striata homogenate (1:9 v/v ratio in 0.32 M sucrose) was used as source for the enzyme. The reaction medium contained striatal homogenate (equivalent to approximately 3 mg of tissue), potassium phosphate buffer (0.5 M, pH 6.0), *m*-hydroxybenzylhydrazine (DOPA decarboxylase inhibitor), 6,7-dimethyl-5,6,7,8-tetrahydropterine (enzymatic cofactor) 1 mM in mercaptoethanol and the test iron chelator at different concentrations (100, 10 and 1 μM). The reaction was initiated by the addition of L-tyrosine 2 mM (final concentration of 0.4 mM), followed by 20 min incubation at 37 °C. The reaction was terminated by the addition of 100 μL perchloric acid 0.4 M containing 5 μM α-methyldopa as internal standard and the mixture was centrifuged for 10 min. L -DOPA and α-methyldopa were extracted onto acid washed alumina (140–150 mg) from 150 μL of the resultant supernatant. Tris buffer (pH 8.6, 1 mL) was added and the mixture was shaken for 10 min. The supernatant was aspirated and the alumina residue washed twice with water. After the second wash, 200 μL of perchloric acid (0.4 M) was added shaking vigorously for 10 min to elute L-DOPA and α-methyldopa from the alumina. The resultant supernatant was used for HPLC analysis to determine the concentration of L-DOPA and α-methyldopa. The assay was performed in triplicate for each chelator. Non–enzymatic formation of L-DOPA was determined by the addition of D-tyrosine and 3-iodotyrosine (tyrosine hydroxylase inhibitor) instead of L-tyrosine. For the HPLC, the mobile phase was 0.1 M sodium phosphate (pH 3.0) containing EDTA (1 mM), octane sulphonic acid (0.65 mM) and 5% methanol. The flow rate was 1 mL/min and the column was a Spherisorb ODS2 (reverse phase chromatography). Quantitation was performed using peak height ratio with the internal standard α-methyldopa.

4.6. Neuroprotection study in cultured mouse cortical neurones

Culture reagents were obtained from Gibco-Invitrogen (UK) and all others chemicals were obtained from Sigma-Aldrich (UK) unless otherwise stated. Primary cultures of cortical neurons were prepared from NIH Swiss white mouse embryos at E15-16 (Harlan, UK). Animal procedures were in accordance with the Home Office, Animals Scientific Procedures Act (1986, UK). Primary cultures of cortical neurons were prepared from E15 mouse embryos on a weekly basis as described previously.[36,28] FeNTA was prepared by mixing a solution of nitrilotriacetic acid disodium salt (Na_2NTA) (1.91 g/100 ml, 100 mM) and a solution of nitrilotriaceticacetic acid trisodium salt (Na_3NTA) (1.9 g/100 ml, 100 mM) at pH 7. The required volume of atomic absorption iron standard solution was added to give a 5:1 molar ratio. A fresh stock solution of 3 mM FeNTA was prepared for each experiment (75 μL NTA, 85 μL iron and 340 μL H_2O), filtered and incubated for 15 min before use, in order to ensure that the compound was in the iron (III) oxidation state before application to cell cultures. The stock solution of the drug was prepared in sterile 100% dimethylsulphoxide (DMSO) and stored at -20 °C until use. Final test concentrations were obtained by diluting in the neuronal culture medium (DMEM-F12) giving a final concentration of 1% DMSO. Human Aβ[1–40] (Cat No. 641-10; Lot: ML0810) was purchased from California Peptides Research (Napa, CA). Aβ was dissolved in DMSO before addition to the cell cultures. Cultured cortical neurons in 24 well plates were treated with different concentrations of FeNTA (3 μM or 10 μM) or Aβ (3, 10 or 20 μM) for 6 h or 30 min, respectively at 37 °C. Following this, the cells were treated with the different chelators (10 μM, 30 μM or 100 μM) or vehicle control. Cells were subsequently incubated for a further 24 h before being assessed for viability or other measures. All experiments were performed in triplicate.

4.7. Cytotoxicity measurements

4.7.1. Lactate dehydrogenase (LDH)

Total LDH release into the culture medium by dead and dying cells (CytoTox-96 LDH assay, Promega, Southampton, UK) was measured. Cells were incubated untreated with 0.1% Triton X-100 for 10 min (37 °C, 5% CO2, 95% air) to induce maximal cell lyses. Absorbance was measured at 490 nm using a Versemax plate reader. Treatment values were then expressed as a percentage of the total LDH release. Background LDH release (media alone) was subtracted from the experimental values. All data from LDH measurements are expressed as % cytotoxicity, where 100% represents maximum toxicity induced ($n = 3$ from quadruplicates).

4.7.2. 3-(4,5-dimethylthiazol-2-yl)-2,5-diphenyltetrazolium-bromide (MTT) turnover

Cell viability was assessed by measuring the levels of MTT, which is a marker of mitochondrial activity.[37] Following exposure of neuronal cultures to Fe-NTA and/or the tested compound, the cultures were washed twice with sterile PBS before the addition of MTT (1 mg/ml) in HEPES-buffered incubation medium (HBM) pH 7.4 (5 mM HEPES, 154 mM NaCl, 4.6 mM KCl, 2.3 mM $CaCl_2$, 33 mM glucose, 5 mM $NaHCO_3$, 1.1 mM $MgCl_2$, 1.2 mM Na_2HPO_4). Following incubation (45 min; 37 °C), MTT solutions were removed, and the formazan product was solubilized in DMSO, and the absorbance recorded at 505 nm using a Versemax plate reader. Data are presented as a percentage relative to their vehicle controls. All data from MTT measurements are expressed as Formazan blue production % of control, considered as 100%, maximum formazan blue formation, ($n = 3$ from quadruplicates).

4.7.3. Microscopic examination

All cultures were examined by phase contrast microscopy (400× magnification Nikon Inverted Eclipse T) to assess cell body and neurite morphology. Representative images were captured using a digital camera (Nikon, Coolpix).

4.7.4. Synaptophysin measurements

Synaptophysin levels were measured in neuronal lysates by immunoblotting. Cell lysates (20 μg) were run on 10% SDS Polyacrylamide gels, transferred to nitrocellulose membranes by semi-dry electroblotting and probed overnight with a polyclonal anti-synaptophysin antibody (Synaptic Systems, 1/2000 dilution). Membranes were incubated with secondary antibody (Chemicon)

for 45 min, washed and protein bands detected using an ECL detection system with Hyperfilm ECL (GE Healthcare). Films were developed using X-ray imaging equipment Mediphot 837 (Fuji, Germany) and quantified using Image J (NIH) .

4.7.5. Propidium iodide (PI) and HOE 33342 (HOE) staining

Propidium iodide and HOE 33342 (2'-(ethoxyphenyl)-5-(4-methyl-1-piperazinyl)-2',5'-bi-1H-benzimidazole HCl) were both purchased from Calbiochem (Nottingham, UK). HOE 33342 (10 μM) and PI (10 μM) (t=15 minutes) were used to stain viable and dead cells, respectively. HOE 33342 binds DNA in viable cells and it is visualised as a blue colour. PI is a membrane impermeable DNA intercalator, which is only able to permeate dying cells. Therefore, it is useful for staining apoptotic or necrotic cells. Viable and dead cells were quantified using an *IN*1000 Cell Analyser (GE Healthcare, UK).

Acknowledgments

The authors thank Professor Bernt Krebs and Dr. Michael Kloskowski for provision of diffractometer access and X-ray structure determination of compound **13f**.

References and notes

1. Strozyk, D; Bush, A. Neurodegenerative Diseases and Metal Ions: Metal Ions in Life Sciences, Sigel, Sigel and Sigel, **2006**, *1*, 427–435.
2. Gaeta, A.; Hider, R. C. *Br. J. Pharmacol.* **2005**, *146*(8), 1041–1059.
3. Liu, Z. D.; Hider, R. C. *Med. Res. Rev*. **2002**, *22*, 26–64.
4. Cherny, R. A.; Atwood, C. S.; Xilinas, M. E.; Gray, D. N.; Jones, W. D.; Mclean, C. A.; Barnham, K. J.; Volitakis, I.; Fraser, F. W.; Kim, Y. S. *Neuron* **2001**, *30*, 665–676.
5. Kaur, D.; Yantiri, F.; Rajagopalan, S.; Kumar, J.; Mo, J. Q.; Boonplueang, R.; Viswanath, V.; Jacobs, R.; Yang, L., et al *Neuron* **2003**, *37*, 899–909.
6. Regland, B.; Lehmann, W.; Abedini, I.; Blennow, K.; Jonsson, M.; Karlsson, I.; Sjögren, M.; Wallin, A.; Xilinas, M.; Gottfries, C. G. *Dement. Geriatr. Cogn. Disord.* **2001**, *12*, 408–414.
7. Bush, A. I. *Trends Neurosci.* **2003**, *26*, 207–214.
8. Oakley, G. P. *JAMA* **1973**, *225*, 395–397.
9. Amit, T.; Avramovich-Tirosh, Y.; Youdim, M. B. H.; Mandel, S. *FASEB Journal.* **2008**, *22*, 1296–1305.
10. Ben-Shachar, D.; Kahana, N.; Kampel, V.; Warshawsky, A.; Youdim, M. B. H. *Neuropharmacology* **2004**, *46*, 254–263.
11. Boddaert, N.; Le Quan Sang, K. H.; Rötlg, A.; Leroy-Willig, A.; Gallet, S.; Brunelle, F.; Sidi, D.; Thalabard, J. C.; Munnich, A.; Cabantchik, Z. I. *Blood* **2008**, *110*, 401–408.
12. Kakhlon, O.; Manning, H.; Breuer, W.; Melamed-Book, N.; Lu, C.; Cortopassi, G.; Munnich, A.; Cabantchik, Z. I. *Blood* **2008**, *112*, 5219–5227.
13. Maggio, A.; D'Amico, G.; Morabito, A.; Capra, M.; Ciaccio, C.; Cianciulli, P.; Di Gregorio, F.; Garozzo, G.; Malizia, R.; Magnano, C., et al *Blood Cell Mol. Dis.* **2002**, *28*, 196–208.
14. Olivieri, N.; Koren, G.; Hermann, C.; Bentur, Y.; Chung, D.; Klein, J.; Louis, S. T. P.; Freedman, M. H.; Mcclelland, R. A.; Templeton, D. M. *Lancet* **1990**, *336*, 1275–1279.
15. Habgood, M. D.; Liu, Z. D.; Dehkordi, L. S.; Khodr, H. H.; Abbott, J.; Hider, R. C. *Biochem. Pharmacol.* **1999**, *57*, 1305–1310.
16. Molina-Holgado, F.; Gaeta, A.; Francis, P.; Williams, R. J.; Hider, R. C. *J. Neurochem.* **2008**, *105*, 2466–2476.
17. Molina-Holgado, F.; Hider, R. C.; Gaeta, A.; Williams, R.; Francis, P. *Biometals* **2007**, *20*, 639–654.
18. Hider, R. C.; Ma, Y.; Molina-Holgado, F.; Gaeta, A.; Roy, S. *Biochem. Soc. Trans.* **2008**, *36*, 1304–1308.
19. Piyamogkol, S.; Liu, Z. D.; Hider, R. C. *Tetrahedron* **2001**, *57*, 3479–3486.
20. Raymond, K. N.; Müller, G.; Matzanke, B. F. *Top Curr. Chem.* **1984**, *58*, 49–102.
21. Hider, R. C.; Singh, S.; Porter, J. B. *Proc. R. Soc. Edinburgh* **1992**, *99B*(1/2), 137–168.
22. Abeysinghe, R. D.; Roberts, P. J.; Cooper, C. E.; MacLean, K. H.; Hider, R. C.; Porter, J. B. *Journal. Biol. Chem.* **1996**, *271*, 7965–7972.
23. Liu, Z. D.; Kayyali, R.; Hider, R. C.; Porter, J. B.; Theobald, A. E. *Journal. Med. Chem.* **2002**, *45*, 631–639.
24. Hider, R. C. *Toxicol. Lett.* **1995**, *82–83*, 961–967.
25. Liu, Z. D.; Lockwood, M.; Rose, S.; Theobald, A. E.; Hider, R. C. *Biochem. Pharmacol.* **2001**, *61*, 285–290.
26. Wagner, K. R.; Sharp, F. R.; Ardizzone, T. D.; Lu, A.; Clark, J. F. *J. Cereb. Blood Flow Metab.* **2003**, *23*, 629–652.
27. Schilling, K.; Barco, E. B.; Rhinehart, D.; Pilgrim, C. *J. Neurosci. Res.* **1989**, *24*, 347–354.
28. Chen, C. X.-Q.; Huang, S. Y.; Zhang, L.; Liu, Y.-J. *Neurobiol. Dis.* **2005**, *19*, 419–426.
29. Whitnall, M.; Richardson, D. R. *Semin. Pediatr. Neurol.* **2006**, *13*, 186–197.
30. Selkoe, D. J. *Ann. N.Y. Acad. Sci* **2000**, *924*, 17–25.
31. Ong, W. Y.; Halliwell, B. *Ann. N.Y. Acad. Sci.* **2004**, *1012*, 51–64.
32. Berg, D.; Youdim, M. B. *Top Magn. Reson. Imaging* **2006**, *17*, 5–17.
33. Liu, D. Y.; Liu, Z. D.; Lu, S. L.; Hider, R. C. *Journal. Chromatogr., B* **1999**, *730*, 135–139.
34. Gans, P.; Sabatini, A.; Vacca, A. *Ann. Chim.* **1999**, *89*, 45–49.
35. Gans, P.; O'Sullivan, B. *Talanta* **2000**, *51*, 33–37.
36. Crossthwaite, A. J.; Hasan, S.; Williams, R. J. *J. Neurochem.* **2002**, *80*, 24–35.
37. Carmichael, J.; DeGraff, W. G.; Gazdar, A. F.; Minna, J. D.; Mitchell, J. B. *Cancer Res.* **1987**, *47*, 936–942.